Versatile Self-Adapting Boronic Acids for H-Bond Recognition: From Discrete to Polymeric Supramolecules

Irene Georgiou,[†] Simon Kervyn,[†] Alexandre Rossignon,[†,§] Federica De Leo,[†] Johan Wouters,[†] Gilles Bruylants,[‡] and Davide Bonifazi*[,†,§]

[†]Department of Chemistry, University of Namur (UNamur), Rue de Bruxelles 61, 5000 Namur, Belgium

[‡]Université Libre de Bruxelles, Ecole Polytechnique de Bruxelles, Campus du Solbosch, Avenue F. D. Roosevelt 50, 1050 Bruxelles, Belgium

[§]School of Chemistry, Cardiff University, Park Place, Main Building, Cardiff CF10 3AT, U.K.

S *Supporting Information*

ABSTRACT: Because of the peculiar dynamic covalent reactivity of boronic acids to form tetraboronate derivatives, interest in using their aryl derivatives in materials science and supramolecular chemistry has risen. Nevertheless, their ability to form H-bonded complexes has been only marginally touched. Herein we report the first solution and solid-state binding studies of the first double-H-bonded DD·AA-type complexes of a series of aromatic boronic acids that adopt a *syn−syn* conformation with suitable complementary H-bonding acceptor partners. The first determination of the association constant (K_a) of *ortho*-substituted boronic acids in solution showed that K_a for 1:1 association is in the range between 300 and 6900 M^{-1}. Crystallization of dimeric 1:1 and trimeric 1:2 and 2:1 complexes enabled an in-depth examination of these complexes in the solid state, proving the selection of the $-B(OH)_2$ *syn−syn* conformer through a pair of frontal H-bonds with the relevant AA partner. Non-*ortho*-substituted boronic acids result in "flat" complexes. On the other hand, sterically demanding analogues bearing *ortho* substituents strive to retain their recognition properties by rotation of the ArB(OH)$_2$ moiety, forming "T-shaped" complexes. Solid-state studies of a diboronic acid and a tetraazanaphthacene provided for the first time the formation of a supramolecular H-bonded polymeric ribbon. On the basis of the conformational dynamicity of the $-B(OH)_2$ functional group, it is expected that these findings will also open new possibilities in metal-free catalysis or organic crystal engineering, where double-H-bonding donor boronic acids could act as suitable organocatalysts or templates for the development of functional materials with tailored organizational properties.
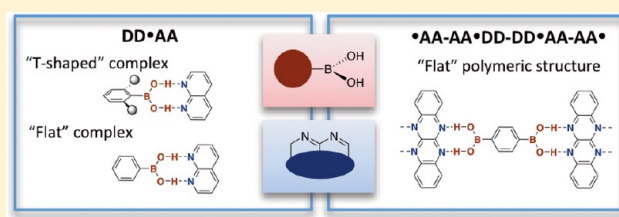
INTRODUCTION

Organoboronic acids are an important group of compounds that have risen to their highest impact since their use in organic synthesis and medicinal chemistry.[1] However, great interest has also recently been reserved for applications in supramolecular chemistry,[2] sensing,[3] and organic catalysis[4] because of the peculiar dynamic covalent reactivity[5] of ArB(OH)$_2$ and its dehydrated derivatives, which enables the engineering of a large variety of architectures resulting from boronate esterification[6] as well as boroxine[7] and spiroborate formation,[8] to name a few.

However, the ability to form H-bonded complexes and their exploitation in molecular recognition has been relatively unexplored.[2] H-bonded architectures are often obtained by exploiting the self-association of organoboronic acids that form polymeric two- and three-dimensional H-bonded architectures in the solid state,[9] with phenylboronic acid being one of the first examples reported.[9,10] In these systems, homodimers are formed and then organized as tapes in which the ArB(OH)$_2$ functionalities adopt a *syn−anti* conformation (Figure 1a), triggering the formation of frontal DA·AD complexes that are held together by lateral intermolecular H-bonds.[10] Diamondoid-like
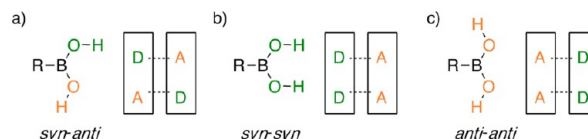
Figure 1. Structural representation of the (a) *syn−anti*, (b) *syn−syn*, and (c) *anti−anti* conformations of the boronic acid RB(OH)$_2$ functionality, adopted when it acts as a DA, DD, and AA system, respectively, in DA·AD, DD·AA, and AA·DD complexes. D and A denote the H-bonding functional group donor and acceptor, respectively.[8−17]

three-dimensional architectures can also be obtained when a tetratopic building block that tetrahedrally exposes four arylboronic acids is used.[11] When a 2-methoxy-substituted ArB(OH)$_2$ is employed, the boronic acid moiety is locked into the *syn−anti* conformation through an intramolecular H-bond involving one hydroxyl group and the oxygen heteroatom situated at the *ortho* position.[12] In the solid state, this restricts the formation of the architectures only to dimers. Similar behavior is

Scheme 1. Schematic Representation of the Possible Non-covalent Complexes Formed between Mono- or Ditopic Boronic Acids and the H-Bond Acceptors NAP and TANP: (a) Discrete 1:1 Complexes; (b) Discrete 2:1 and 1:2 Complexes; (c) a Supramolecular Polymer[a]
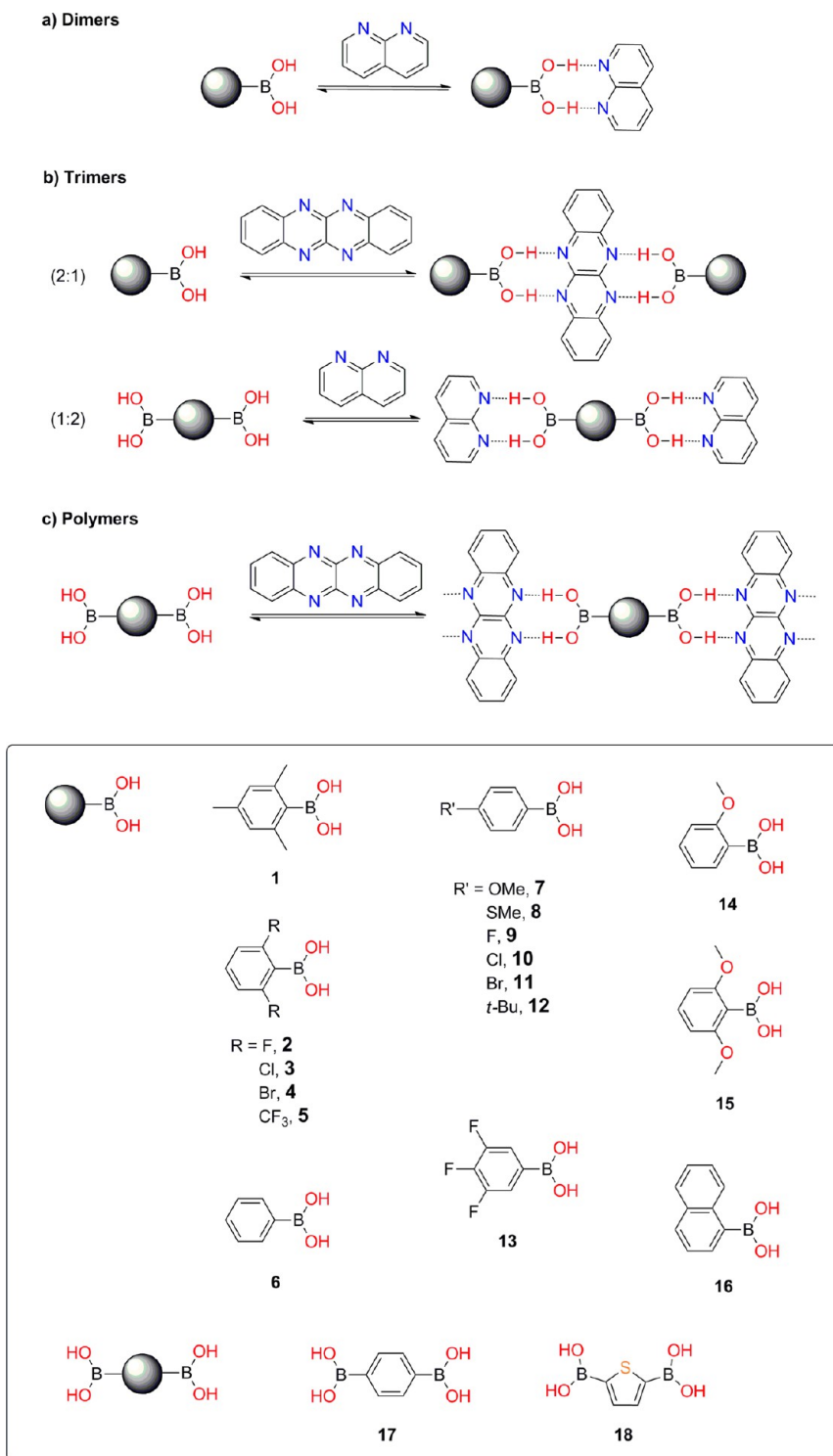
[a]All of the boronic acids were purchased, except for **14**, which was prepared following a literature protocol.[21b]

observed for *ortho*-substituted $ArB(OH)_2$ bearing an imino, aminomethyl, or azo group.[13] Weak intramolecular H-bonds are also observed in the presence of fluorine atoms.[14] On the other hand, when a 2,6-dimethoxy-substituted $ArB(OH)_2$ is used, the hydroxyl groups adopt an *anti−anti* conformation (Figure 1c), which disfavors the formation of intermolecular H-bonds, thus

leading to monomeric species in the solid state.[12b,15] The *anti−anti* conformation can be also observed in the solid state in cocrystals containing either urea derivatives[16a] or carboxyl groups.[16b] Finally, the *syn−syn* $ArB(OH)_2$ conformation is seldom observed in DD·AA type complexes, being essentially restricted to cocrystals containing carboxylates,[17a−d] bis-pyridine,[17e−i] or

1,10-phenanthroline and 1,2-diazaheteroaromatics[17j] (Figure 1b). In a very recent work it was postulated that the *syn−syn* conformer of a variety of ArB(OH)$_2$ is the active catalytic species in the fixation of CO$_2$ with epoxides to give the corresponding cyclic carbonates in excellent yields.[18]

Although the evidence for the formation of H-bonded boronic acids is substantial and its relevance in the solid state has been essentially limited to self-associated architectures, data regarding the thermodynamics of the interactions with complementary recognition motifs in solution are essentially unknown. With the desire to explore the potential of boronic acids as self-adapting H-bonding recognition molecular modules, this paper focuses on the study of the association capabilities of ArB(OH)$_2$ to form DD·AA-type heterocomplexes in which the H-bonding donor hydroxyl groups adopt a *syn−syn* conformation. This can be considered as a dynamic mimic of bicyclic guanidinium binding modules.[19] On the basis of Jorgensen's model[20] of multiple H-bonding systems, the proposed DD·AA heteromolecular complexes should display enhanced stability as a consequence of the favorable secondary interactions. In identifying suitable complementary AA acceptors, we were drawn to 1,8-naphthyridine (**NAP**), whose N···N distance of 2.403 Å structurally matches the conformational properties of *syn−syn* boronic acid (Scheme 1). In addition, its easy synthetic accessibility and the prospect of preparing an acceptor partner featuring multiple AA moieties (AA−AA), such as 5,6,11,12-tetraazanaphthacene (**TANP**),[21a] provided opportunities to further investigate discrete and polymeric architectures with suitably tailored boronic acids (Scheme 1) and thus the construction of supramolecular H-bonded architectures.[22] Hence, we started with an examination of dimeric 1:1 (DD·AA) complexes involving *syn−syn* boronic acids and **NAP** (Scheme 1a). In particular, the successful detection and quantification of the complexation in solution and in the solid state was first complemented by computational predictions and then experimentally proven. Reference studies with 1,10-phenanthroline (**Phen**) were also performed and showed a similar DD·AA complexation behavior, in agreement with a literature report[17j] describing heteromolecular dimeric complexes with 4-bromo-, 4-hydroxy-, and 3-methoxyphenylboronic acid. Furthermore, a series of crystal structures of trimeric 2:1 and 1:2 complexes (i.e., DD·AA−AA·DD and AA·DD−DD·AA, respectively) were also obtained and examined (Scheme 1b), showing the versatility of the recognition motif to build defined supramolecules. Finally, a procedure leading to the formation of crystals of the first supramolecular H-bonded polymeric network, (AA−AA·DD−DD)$_n$, involving a diboronic acid (DD−DD) and a suitable ditopic acceptor (AA−AA) was developed (Scheme 1c).

■ RESULTS AND DISCUSSION

Computational Modeling of the Conformational Properties of Phenylboronic Acid and Its Aptitude To Form DD·AA Complexes. In the literature, the relative energies of the three conformations a boronic acid moiety can adopt have been calculated, revealing a minor energy difference between them (< ∼ 3 kcal mol^{-1}). The first report based its theoretical calculations on the substrate where the substituent is a hydrogen atom,[23] and this was later followed by the phenylboronic acid analogue.[17j] In both cases, the *syn−anti* conformation is the most favorable, since the repulsion of the two positively charged hydrogen atoms is minimized. This is in accordance with the large number of crystal structures where the boronic acid moiety self-interacts in a *syn−anti* fashion.[10−15] In line with the above-mentioned literature reports, through density

functional theory (DFT) calculations performed at the B3LYP/6-311G** level, we also found that the *syn−anti* geometry is the most favorable conformation compared with the *syn−syn* (−2.20 kcal mol^{-1}) and *anti−anti* (and −2.82 kcal mol^{-1}) arrangements for phenylboronic acid (Figure 2, upper panel).
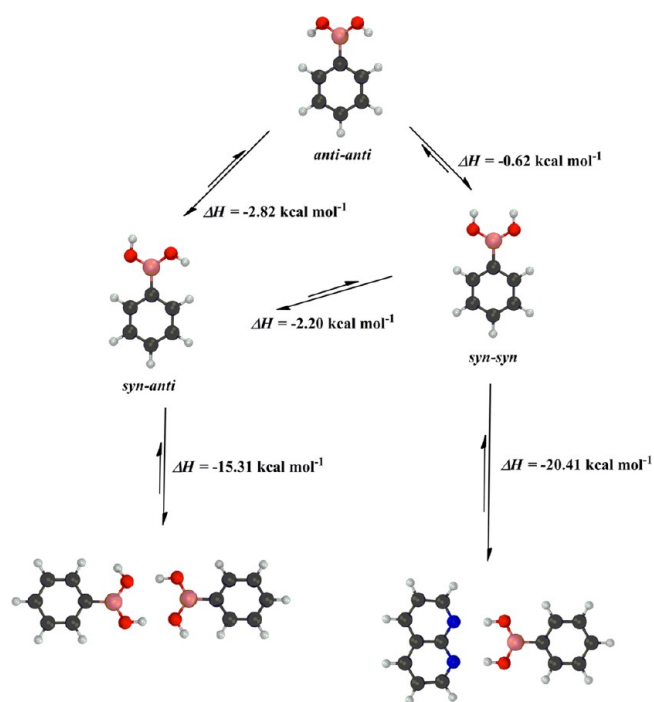

Figure 2. Calculated geometries and enthalpies for the three different conformations of phenylboronic acid (i.e., *syn−syn*, *anti−anti*, and *syn−anti*) and of the homo- and heterodimers (B3LYP/6-311G**, Gaussian 09). Red = oxygen, blue = nitrogen, pink = boron, white = hydrogen, and black = carbon.

The low-ranked *anti−anti* conformation is also accompanied by a loss of planarity essentially caused by steric hindrance between the hydrogen atoms of the hydroxyl groups and the *o*-H atoms of the phenyl ring (Figure 2). In order to gain information about the association capabilities with **NAP** with respect to the dimerization equilibrium between the single boronic acids, a comparative DFT analysis in vacuum was carried out. In particular, a theoretical estimation of the enthalpy of complexation between phenylboronic acid and **NAP** was performed, considering the three conformational equilibria as well as the phenylboronic acid homodimerization equilibrium as references. As shown in bottom panel of Figure 2, the homodimerization of phenylboronic acid (ΔH = −15.31 kcal mol^{-1}) is not negligible compared with the small energy difference between the three conformations. Nevertheless, the formation of the DD·AA heterodimer with **NAP** is energetically favored (ΔH = −20.41 kcal mol^{-1}) with respect to the formation of the DA·AD homodimer, supporting the idea that the **NAP** scaffold is a suitable preorganized H-bonding AA partner for the formation of DD·AA complexes with enhanced thermodynamic stabilities.

Determination of the Heteromolecular Association Constant in Solution (K_a) by NMR and ITC Investigations. Because of the fast hydrogen atom exchange that usually occurs in solution with acidic protons, the proton resonances of a boronic acid are usually not observed in most of the cases where CDCl$_3$ is used as the solvent. In contrast, when toluene-d_8 is used, a sharp peak fingerprinting the acidic ArB(OH)$_2$ protons appears

between 3.5 and 4 ppm (Figure 3a). Prior to the discussion of the heteromolecular binding results, a careful examination of the
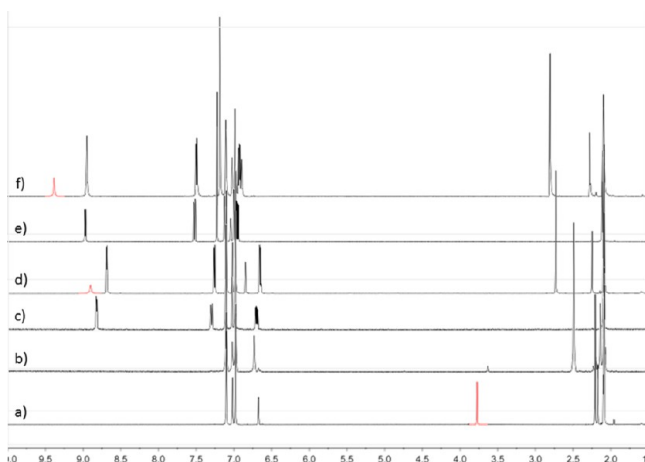

Figure 3. Selected region of the ^{1}H NMR spectra (500 MHz, toluene-d_8, 298 K) of (a) mesitylboronic acid (**1**), (b) mesitylboroxine, (c) **NAP**, (d) the 1:1 **1·NAP** complex, (e) **Phen**, and (f) the 1:1 **1·Phen** complex.

chosen experimental conditions is necessary, as arylboronic acids can be involved in other equilibria besides that of the AA·DD complex (Scheme 2). In particular, boronic acids are known to be

Scheme 2. Chemical Equilibria Involving a Boronic Acid in Solution: Formation of the Non-covalent AD·DA-Type Homodimer (K_d) and the DD·AA Heterodimer (K_a), the Boroxine (K_{borox}), and Hydroxyboronate Ions (K_i)
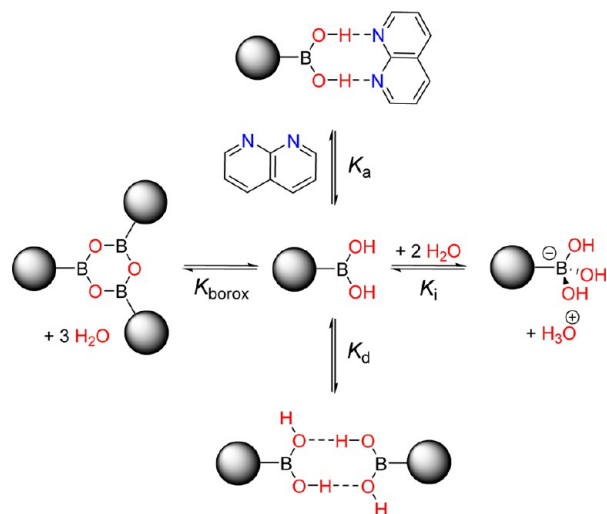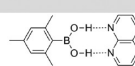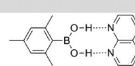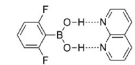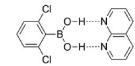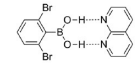

in equilibrium with their cyclic anhydride (boroxine) forms (K_{borox}).[24] The equilibrium between the acid and anhydride forms in solution mainly depends on the temperature and on the position of the aryl substituents, with the derivatives bearing *ortho* substituents being kinetically more stable, exclusively existing as acids in solution at room temperature, compared with the *para* analogues, which are often found as mixtures.[1,24b] Thus, to avoid the presence of the boroxine form, only *ortho*-substituted ArB(OH)$_2$ derivatives were used to estimate the homoassociation constants in solution (as one can see from Figure 3b, the presence of the boroxine form can easily be diagnosed by ^{1}H NMR analysis using the fingerprinting Ar–H
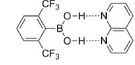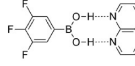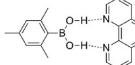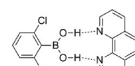
resonances). Next, the homodimerization constants (K_d) for the relevant boronic acids were also measured. Dilution experiments revealed K_d values lower than 10 M^{-1} in toluene-d_8 (see the dilution ^{1}H NMR experiments in the Supporting Information (SI)), suggesting that the homodimerization equilibrium has a negligible effect on the heteroassociation with either **NAP** or **Phen**. This is in line with the literature reports describing other weakly H-bonded AD·DA-type homodimers.[25] Finally, the effect of water was studied, as the formation of hydroxyboronate ions (K_i) could affect the determination of the heteromolecular association constant as a result of the structural change of the functional group from a trigonal-planar structure to a tetrahedral structure.[26] Although the addition of successive aliquots of H$_2$O did not show any appreciable change in the chemical shift of the boronic acid O*H* proton resonances in the ^{1}H NMR spectrum taken in toluene-d_8 (see the SI), it is known that fast chemical exchange[27] between the trigonal-planar boronic acid and the tetrahedral hydroxyboronate ion is present. Because of the nature of this fast equilibrium, the diagnostic ^{11}B and ^{1}H resonances fingerprinting the hydroxyboronate and boronate groups under neutral pH conditions are not detected. However, considering that the ^{11}B resonances for all of the boronic acids investigated in this work are centered at ca. 30 ppm,[27a] we cannot entirely exclude the presence of tetrahedral hydroxyboronate ions. Low-temperature ^{1}H NMR experiments were also performed to investigate the existence of any H-bonding interactions between the boronic acid O*H* protons and the water molecules. Again, no direct evidence of any H-bonding interactions between these two molecules were observed (see the SI). Hence, to ensure the same experimental conditions for the binding studies with the relevant boronic acids and acceptors, the ratio of the boronic acid content to the H$_2$O content was kept constant in all of the solutions.

Given these experimental premises, the H-bonding DD-type self-adaptability of arylboronic acids toward association with a suitable AA acceptor (**NAP** or **Phen**) was systematically studied by considering different derivatives (listed in Table 1) for the first time through ^{1}H NMR titration experiments. Titration experiments (Figure 4a; also see the SI) showed a fast association equilibrium involving a progressive downfield shift of the diagnostic boronic acid O*H* resonances for all of the derivatives (Table 1, **1–5**) upon incremental addition of **NAP** (e.g., the δ_H of the O*H* shifts from 3.77 to 9 ppm for the **1·NAP** complex; Figure 4a). Through free-concentration nonlinear least-squares curve fitting,[28] for which the initial concentration of the boronic acid was also considered as a variable (C_0'), the association constants (Table 1 and Figure 4b) were found to be 369 ± 16, 997 ± 62, 1465 ± 66, 903 ± 41, and 6900 ± 760 M^{-1} for complexes **1·NAP**, **2·NAP**, **3·NAP**, **4·NAP**, and **5·NAP**, respectively, all of which display a 1:1 stoichiometry (as evidenced by Job plot analysis; that of **1·NAP** is shown in Figure 4c). The K_a values are in line with those of other AA·DD complexes reported in the literature.[20c,29] As one can notice, the fitted C_0' is always lower than that supposed experimentally, namely, C_0 = 0.01 M. It is likely that this can be ascribed to the presence of the hydroxyboronate formation equilibrium (see the above discussion), which significantly reduces the real concentration of the boronic acid in solution. Although only a 15% yield of boroxine was observed for solutions containing 3,4,5-trifluorophenylboronic acid (as estimated by ^{1}H NMR analysis based on the aromatic proton resonance at 7.40 ppm), attempts to measure the association constant for this phenylboronic acid and **NAP** by NMR titration proved to be fruitless because the peak finger-printing the OH resonance overlapped with the solvent resonance,

Table 1. Association Constant (K_a) Values Determined by NMR Titrations and ITC for Complexation of the Relevant Substituted Arylboronic Acids to NAP and Phen in Toluene-d_8 at 295 K[e]

Complex	$K_a{}^a$	$C_0{}^{,b}$	$K_a{}^a$	ΔH^{0c}	$-T\Delta S^{0c}$	n
	NMR		ITC			
1·NAP	369 ± 16	9.2	300 ± 60	-8.9 ± 0.3	5.5 ± 0.5	0.95 ± 0.05
2·NAP	997 ± 62	8.7	750 ± 100	-10.5 ± 0.5	6.7 ± 0.5	1 ± 0.05
3·NAP	1465 ± 66	8.7	1100 ± 200	-11.7 ± 0.5	7.4 ± 0.5	0.97 ± 0.08
4·NAP	903 ± 41	7.7	1700 ± 200	-9.3 ± 0.3	5.0 ± 0.3	0.82 ± 0.04
5·NAP	6900 ± 760	8.7	4600 ± 500	-10.5 ± 0.5	6.7 ± 0.5	0.9 ± 0.1
13·NAP	-[d]	-[d]	18000 ± 2500	-11.7 ± 0.3	7.4 ± 0.5	1 ± 0.01
1·Phen	769 ± 35	1.0	-[d]	-[d]	-[d]	-[d]
3·Phen	2306 ± 79	8.8	-[d]	-[d]	-[d]	-[d]

^{a}In M^{-1}. ^{b}In mM. ^{c}In kcal mol^{-1}. ^{d}Not measured. ^{e}Values obtained by NMR titrations were calculated through a free-concentration fitting approach of a 1:1 binding isotherm, where the initial concentration of the boronic acid was also considered as a variable (C_0') that was calculated consequently. The uncertainty in K_a was estimated from two or three independent runs. Thermodynamic parameters derived from ITC experiments represent means of the values obtained by fitting of a 1:n binding isotherm to three independent experiments, and the reported errors represent the 95% confidence intervals.

thus preventing an accurate estimation of the chemical shift values (see the SI). 2,6-bis(trifluoromethyl)phenylboronic acid did not form any boroxine in toluene but its OH resonance peak became extremely broad during the titration experiments. Model titration experiments were also performed in other solvents (CD_2Cl_2 and CD_3CN) with boronic acid **3** and **NAP** as the donor and acceptor molecules, respectively, to study the effect of the solvent polarity on the 1:1 association strength. As expected, solvents with increasing dielectric constants cause a progressive decrease in the strength of the H-bonding interaction,[30] with the association constants K_a(solvent) being the following: 1465 ± 66 in toluene ($\varepsilon = 2.38$), 1234 ± 54 in CD_2Cl_2 ($\varepsilon = 8.93$), and 10.94 ± 0.48 in CD_3CN ($\varepsilon = 37.5$).

Similar results were also obtained by complementary ITC titrations, even if the values are approximately and systematically 20% lower than those measured by NMR titration. It is worth mentioning that except for the **13·NAP** and **5·NAP** complexes, the association constants are in the lower range of values accessible by ITC and could only be measured thanks to the high solubility of both the host and guest molecules in toluene. The trend observed in the K_a values is the same for both methods, i.e., an increased affinity for the boronic acid derivatives bearing electron-withdrawing groups. As expected, the increased affinity is predominantly of enthalpic origin, as confirmed by the $\Delta H°$ values reported in Table 1. Specifically, complex **1·NAP** displays a less favorable interaction enthalpy and affinity constant, whereas the most favorable values are obtained for complex **13·NAP**, which is the only complex not bearing *ortho* substituents and the only one showing a "flat" geometry. Reference titration experiments (see the SI) with 2-methoxyphenylboronic acid (**14**), in which the boronic acid OH protons are preferentially

locked in the *syn*−*anti* conformation through an intramolecular H-bonding interaction established with the methoxy group, did not show any significant downfield shift of the OH resonances. This suggests that no complex is formed when the characteristic conformational dynamicity of the boronic acid recognition group is lost.

Having determined the K_a values for 1:1 molar ratio complexes, we also attempted to study the formation of trimeric complexes in solution (Scheme 1b). Unfortunately, the scarce solubility of the ditopic molecular modules (i.e., 1,4-diphenyleneboronic acid (**17**), 2,5-thiophenediboronic acid (**18**), and **TANP**) in toluene hampered an accurate determination of the thermodynamic properties of the involved equilibria. However, when CD_2Cl_2 was used, we could estimate the association strengths of boronic acids with **TANP** because of its solubility in chlorinated solvents. In particular, using boronic acid **3** as suitable DD molecular partner, a 2:1 association equilibrium could be probed with **TANP** as the acceptor. Two weak association constants were measured, namely, $K_{a1} = 126 \pm 2$ M^{-1} and $K_{a2} = 29 \pm 1$ M^{-1} for the formation of the 1:1 (i.e., **3·TANP**) and 2:1 (i.e., **3·TANP·3**) complexes, respectively. The weak association strengths are not surprising given the low basicity of this kind of aromatic heterocycle. To our surprise, when the AA partner was changed to **Phen**, a significant enhancement of the association constants for complexes **1·Phen** and **3·Phen** was observed (769 ± 35 and 4953 ± 54 M^{-1}, respectively) compared with the **NAP** complexes (369 ± 12 and 1465 ± 66 M^{-1}, respectively). A careful analysis of the computed electronic surface potential (ESP) (see the SI) suggests that the stronger association with **Phen** can be reasonably attributed to stronger favorable secondary electrostatic N···H interactions arising from the shorter
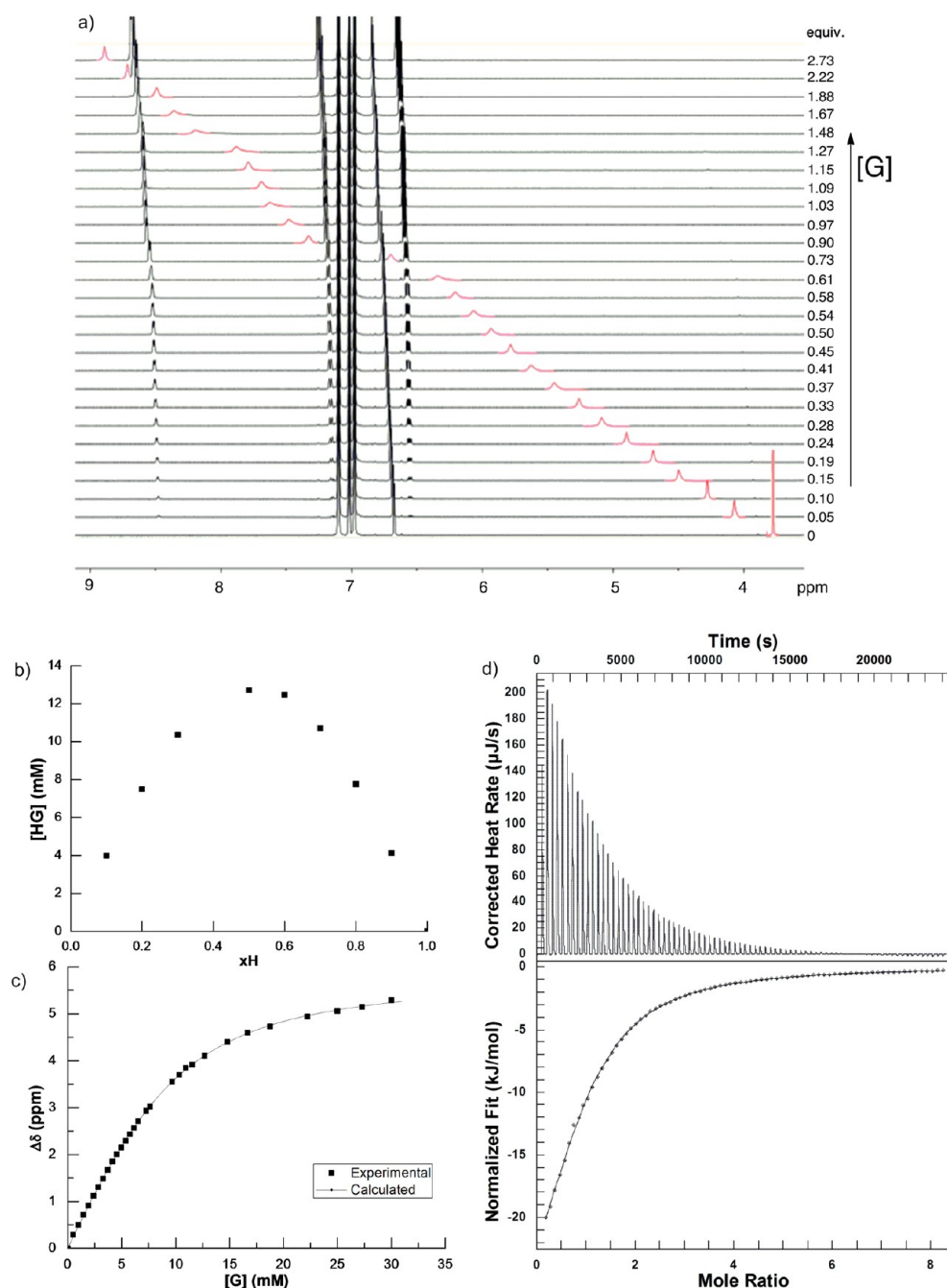
Figure 4. (a) Selected region of a series ^{1}H NMR spectra acquired during the titration of boronic acid **1** with **NAP** (500 MHz, toluene-d_8, 298 K). The concentration of the initial boronic acid was $C_0 = 0.01$ M. (b) Binding isotherm for the formation of the 1:1 complex ($[H]_0 = [1]_0 = 10$ mM; $[G]_0 = [NAP]_0 = 50$ mM; $\Delta\delta_{sat} = 5.23$; $K_a = 369 \pm 16$). (c) Job plot confirming the formation of the 1:1 **1·NAP** complex ($[H]_0 + [G]_0 = 5$ mM, xH = $[H]_0/([H]_0 + [G]_0)$). (d) ITC data for the titration of boronic acid **1** (4.9 mM) with **NAP** (200 mM) in toluene at 298 K.

interatomic N···H distances resulting from the peculiar arrangement of the N atoms in the phenanthroline scaffold.

Computational Modeling of the Structural and Association Energies of the DD·AA Complexes. To shed further light on the electronic and conformational properties ruling the formation and stability of the different heteromolecular complexes, DFT geometry optimization and frequency calculations were carried out in vacuum at the B3LYP/6-311G** level using Gaussian 09 (see SI-1). Starting from the reference phenylboronic acid (**6**) (Table 2), it was confirmed that the *syn−anti* conformation is the most favored, with the *syn−syn* conformation 2.2 kcal mol^{-1} higher in energy and adopting an

"in-plane" conformation with the phenyl ring, in contrast to the *anti−anti* conformation, which is highest in energy and "out-of-plane". A similar trend where the *syn−anti* > *syn−syn* > *anti−anti* ranking is noted in the cases of *para*-substituted derivatives bearing electron-withdrawing groups (EWGs) (Table 2, acids **7**, **8**, and **13**). On the other hand, the stability ranking changes to make *anti−anti* as the second-favored conformation after *syn-anti* in derivatives **9**, **3**, and **1**. Among these, derivatives **3** and **1** found a better accommodation in an "out-of-plane" rotamer as a result of the steric hindrance of the substituents in both *ortho* positions. A small energy barrier of about 1.5 kcal mol^{-1} exists between the *anti−anti* and *syn−anti* conformations, while more considerable

Table 2. Theoretical Calculations at the B3LYP/6-311G Level for Different Phenylboronic Acid Derivatives Bearing Substituents at Different Positions: ΔΔH Values for the *syn−syn* and *anti−anti* Conformations Relative to the *syn−anti* Conformation, Dipole Moments (μ), Electrostatic Potential (ESP) Values Corresponding to the Acidic Hydrogen, and Values of ΔH for the Formation of the AA·DD Complexes Involving NAP Are Shown**

#	Substituent					*syn-syn* ΔΔH [a]	*anti-anti* ΔΔH [a]	μ [b]	ESP [c]	Heterodimer ΔH [d]
	R^1	R^2	R^3	R^4	R^5					
6	H	H	H	H	H	2.20 (in)	2.82 (out)	2.44	125.50	-20.41
7	H	H	OMe	H	H	2.07 (in)	2.82 (out)	2.56	134.16	-19.91
8	H	H	SMe	H	H	2.01 (in)	2.89 (out)	3.57	131.77	-20.41
13	H	F	F	F	H	1.38 (in)	3.99 (in)	0.003	119.22	-22.48
9	H	H	F	H	H	1.81 (in)	1.35 (out)	3.96	136.17	-20.95
3	Cl	H	H	H	Cl	3.39 (out)	1.69 (out)	1.55	112.95	-21.79
1	Me	H	Me	H	Me	3.38 (out)	1.32 (out)	3.18	100.40	-20.44
2	F	H	H	H	F	5.84 (out)	-0.38 (in)	2.09	122.36	-21.59
15	OMe	H	H	H	OMe	5.82 (out)	-3.26 (in)	0.91	90.99	-18.67

[structure diagram: B(OH)₂ substituted benzene ring labeled R₁–R₅]

[a]ΔΔH calculated relative to the *syn−anti* conformation, in kcal mol⁻¹; "in" and "out" stand for the "in-plane" and "out-of-plane" conformations, respectively, adopted by the boronic acid moiety with respect to the aromatic plane of the aryl ring. [b]In D. [c]In kcal mol⁻¹. [d]ΔH calculated relative to the free-complex *syn−syn* conformation, in kcal mol⁻¹.

energy barriers have to be overcome to reach the *syn−syn* arrangement. Moving to the *ortho*-substituted derivatives **2** and **15**, it can be seen that the presence of other EWGs besides chlorine, such as fluorine, lead to weak intramolecular H-bonds, with a OH···F distance of 1.95 Å, the latter stabilizing the *anti−anti* conformation as the most favored, although with a very low difference in energy (0.38 kcal mol⁻¹ more stable than *syn−anti*). On the contrary, a considerable difference in energy is detected when the *syn−syn* conformation has to be adopted (5.84 kcal mol⁻¹). Most importantly, the enthalpy of dimerization was computed for each of these derivatives coupled with **NAP**. In comparison with the reference **6**, all of derivatives showing the *syn−syn* conformation as the second most favored exert a consistent ΔH of dimerization that ranges from about −20 to −22 kcal mol⁻¹. Interestingly, the poor stability of the *syn−syn* conformation observed in derivatives **9**, **3**, and **1** does not affect their ability to form stable complexes with **NAP**, which instead exhibit affinity values comparable to those of **6**. Hence, despite the relative stabilities of the three conformations the phenylboronic acid derivatives can adopt, the formation of the heterocomplexes is never compromised, except in the case of molecule **15**, where only the *anti−anti* conformation is present because of the intramolecular H-bonds established with the *o*-methoxy substituents. To appraise the H-bond-donating character, we used the ESP localized on the acidic OH hydrogen atoms (Table 2). By changing the electronic properties of the substituents, variations of the ESP were observed (see SI), with lower and higher values when electron-donating groups (EDGs) and EWGs are present, respectively.

Solid-State Recognition and Supramolecular Organization. Aiming to study the formation of the doubly H-bonded complexes in the solid state as well, we cocrystallized a large variety of arylboronic acids with the selected H-bond acceptor partners **NAP**, **Phen**, and **TANP**. In this case, *ortho*- and *para*-substituted arylboronic acids **1−16** and arylbis(boronic acid) derivatives **17** and **18** were used to form oligomeric and polymeric structures with the relevant H-bond acceptor partners.

As predicted by the theoretical simulations and suggested by the NMR investigations in solution, we expected the boronic acids to self-adapt in a *syn−syn* conformation, forming "T-shaped" or "flat" complexes depending on the presence or absence of *ortho* substituents, respectively (Figure 5). Therefore, parameters such
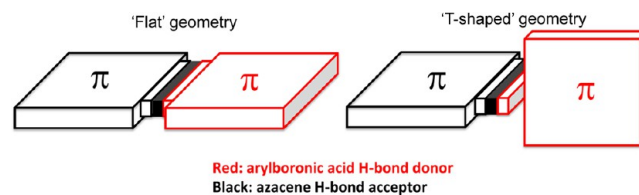

Figure 5. Representations of the "flat" and "T-shaped" complexes.

as the stoichiometry and geometry of the complex, the H-bond distance, and the dihedral angle between the complexed boronic acid moiety and the aryl ring will be the subject of discussion in this section. Notably, in all of the X-ray studies only the crystal structures of the heteromolecular complexes were observed, and no crystals of the free acids or boroxine forms were detected. Surprisingly, this was also the case for those boronic acids known to easily undergo anhydride formation, namely, the *para*-substituted derivatives.[23]

Dimeric "Flat" Complexes. Cocrystallization of phenylboronic acid with **NAP** gave the 1:1 molar ratio dimeric complex **6·NAP** in the solid state (Figure 6a), where the N atoms are frontal to the O atoms. The two N atoms in the AA partner act as H-bond acceptors, and the boronic acid moieties are suggested to adopt a *syn−syn* conformation, thus yielding a pair of H-bonds with N₂···O₂ and N₁···O₁ distances of 2.823 and 2.828 Å, respectively. In addition, the B(OH)₂ moiety is almost coplanar with the phenyl ring, as the O₁−B₁−C₁−C₆ torsion angle is only 3.9°. In the three-dimensional arrangement, the dimeric complexes are held together by π−π interactions, where each **NAP** stacks antiparallel on a phenyl ring (3.509 Å). Similar observations are noted in the cases of **NAP** complexes with naphthalene-1-boronic acid (**16**) and 4-*tert*-butylphenylboronic acid (**12**)
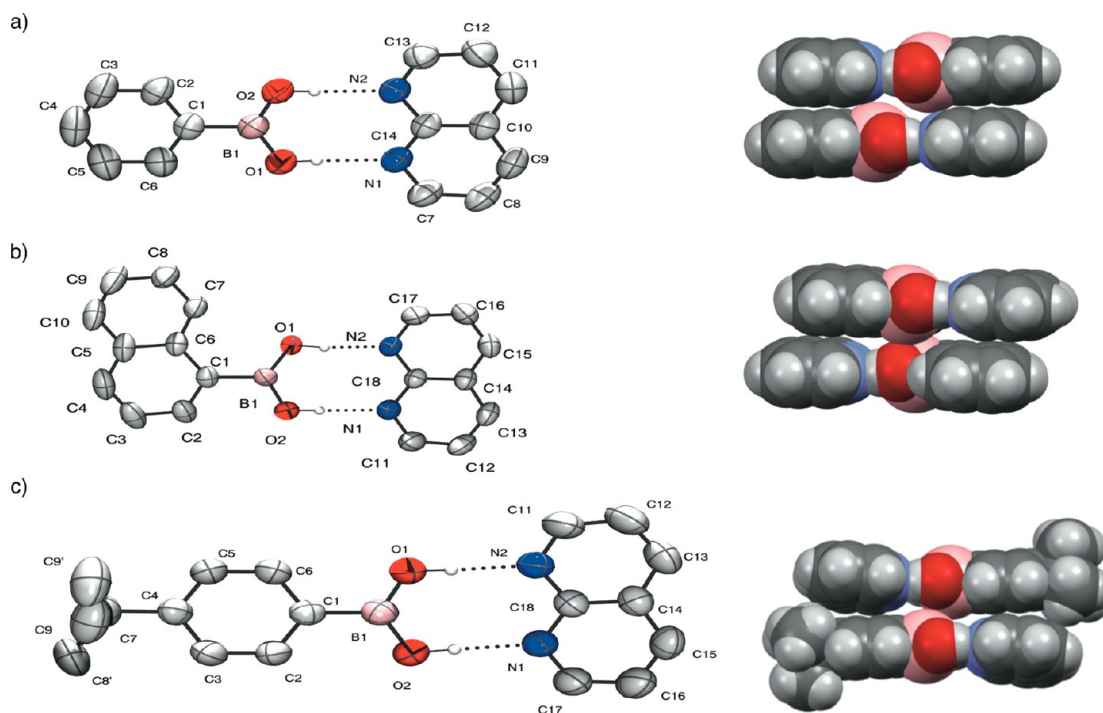
Figure 6. Crystal structures of the dimeric complexes (a) **6·NAP**, (b) **16·NAP**, and (c) **12·NAP**: (left) ORTEP representations drawn at the 30% probability level; (right) space-filling representations. Distances of the H-bonds: (a) $N_2 \cdots O_2$ 2.823(2) Å, $N_1 \cdots O_1$ 2.828(2) Å; (b) $N_2 \cdots O_1$ 2.792(3) Å, $N_1 \cdots O_2$ 2.833(4) Å; (c) $N_2 \cdots O_1$ 2.786(3) Å, $N_1 \cdots O_2$ 2.843(3) Å. Dihedral angles between the aryl and boronic acid groups: (a) $O_1-B_1-C_1-C_6$ 3.9(3)°, $O_1-B_1-C_1-C_2$ 2.6(3)°; (b) $O_1-B_1-C_1-C_6$ 3.5(4)°, $O_1-B_1-C_1-C_2$ 4.3(4)°; (c) $O_1-B_1-C_1-C_6$ 3.7(3)°, $O_1-B_1-C_1-C_2$ 4.6(3)°. Space groups: (a) $P2_1/c$; (b) $P2_1/n$; (c) $P2_1/c$.
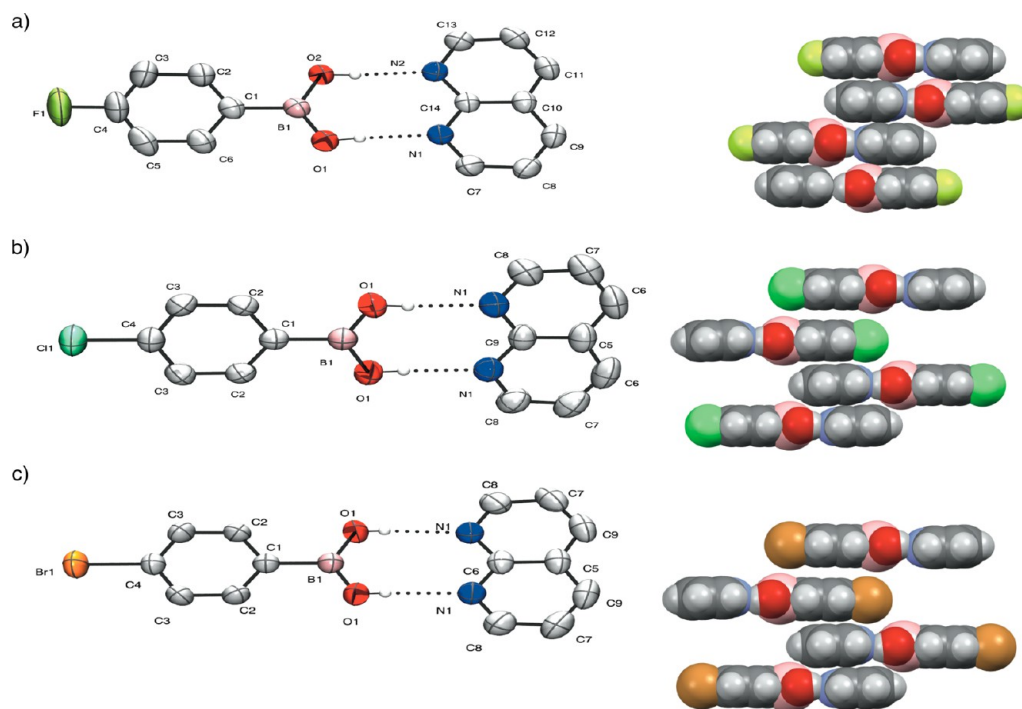

Figure 7. Crystal structures of the dimeric complexes (a) **9·NAP**, (b) **10·NAP**, and (c) **11·NAP**: (left) ORTEP representations drawn at the 30% probability level; (right) space-filling representations. Distances of the H-bonds: (a) $N_2 \cdots O_2$ 2.8250(19) Å, $N_1 \cdots O_1$ 2.8273(18) Å; (b) $N_1 \cdots O_1$ 2.825(2) Å; (c) $N_1 \cdots O_1$ 2.825(3) Å. Dihedral angles between the aryl and boronic acid groups: (a) $O_2-B_1-C_1-C_2$ 1.3(2)°, $O_1-B_1-C_1-C_6$ 0.93(2)°; (b) $O_1-B_1-C_1-C_2$ 0.5(3)°; (c) $O_1-B_1-C_1-C_2$ 0.8(6)°. Space groups: (a) $P2_1/c$; (b) $C2/m$; (c) $C2/m$.

(Figure 6b,c), with the latter displaying a slightly longer $\pi-\pi$ stacking distance (3.797 vs 3.546 Å), most likely caused by the presence of the hindering *p-tert*-butyl substituent.

To investigate further the effect of the *para* derivatization, cocrystals of a series of *para*-substituted phenylboronic acids were analyzed, beginning with the halogen-bearing analogues
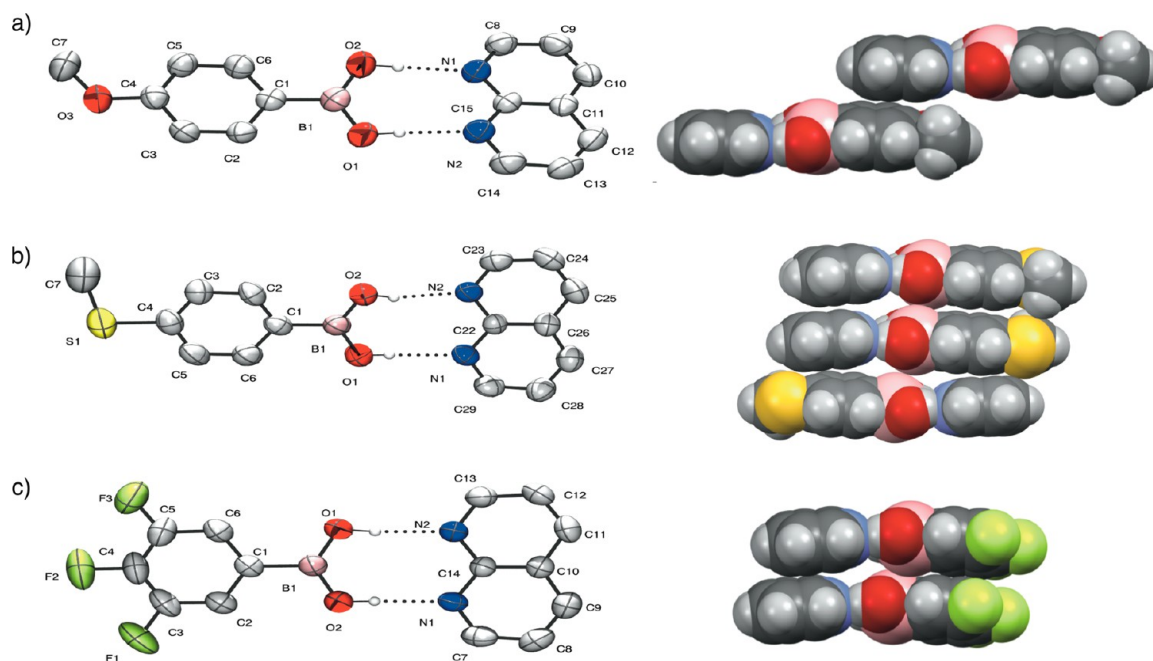
Figure 8. Crystal structures of the dimeric complex (a) **7·NAP**, (b) **8·NAP** and (c) **13·NAP**: (left) ORTEP representations drawn at the 30% probability level; (right) space-filling representations. Distances of the H-bonds: (a) $N_2 \cdots O_1$ 2.819(2) Å, $N_1 \cdots O_2$ 2.845(19) Å; (b) $N_1 \cdots O_2$ 2.837(4) Å, $N_2 \cdots O_2$ 2.811(5) Å; (c) $N_2 \cdots O_1$ 2.820(3) Å, $N_1 \cdots O_2$ 2.829(3) Å. Dihedral angles between the aryl and boronic acid groups: (a) $O_1-B_1-C_1-C_2$ 10.0(2)°, $O_2-B_1-C_1-C_6$ 8.1(2)°; (b) $O_1-B_1-C_1-C_6$ 1.9(7)°, $O_2-B_1-C_1-C_2$ 0.8(6)°; (c) $O_1-B_1-C_1-C_2$ 2.99(4)°, $O_2-B_1-C_1-C_6$ 2.5(4)°. Space groups: (a) $P2_1/c$; (b) $Pbcn$; (c) $P2_1/c$.
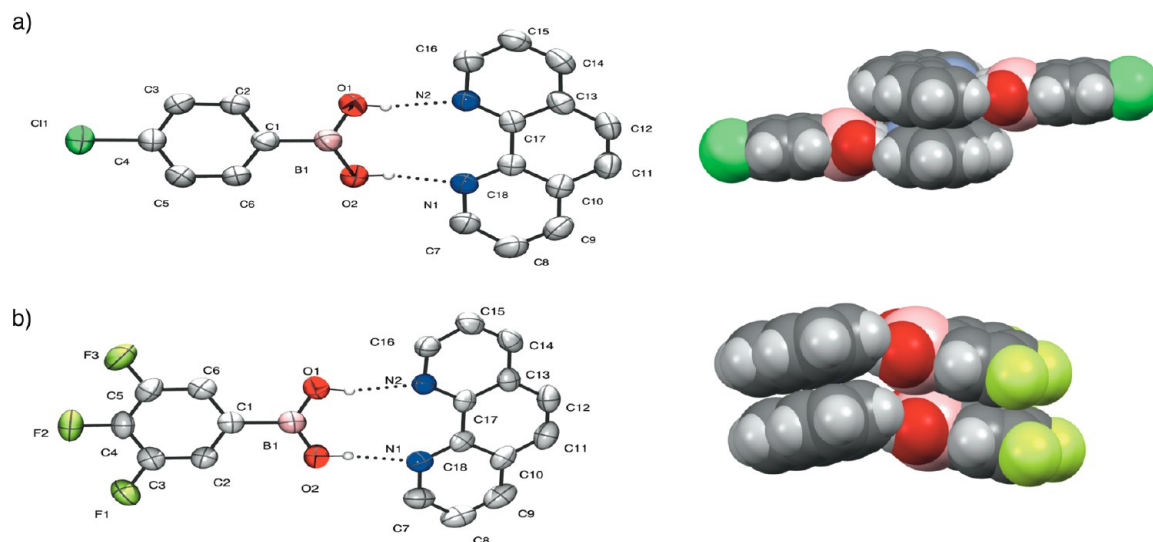

Figure 9. Crystal structures of the dimeric complexes (a) **10·Phen** and (b) **13·Phen**: (left) ORTEP representations drawn at the 30% probability level; (right) space-filling representations. Distances of the H-bonds: (a) $N_2 \cdots O_1$ 2.834(2) Å, $N_1 \cdots O_2$ 2.750(2) Å; (b) $N_1 \cdots O_2$ 2.791(4) Å, $N_2 \cdots O_1$ 2.801(4). Dihedral angles between the aryl and boronic acid groups: (a) $O_1-B_1-C_1-C_2$ 1.9(3)°, $O_2-B_1-C_1-C_6$ 3.40(3)°; (b) $O_1-B_1-C_1-C_6$ 3.8(5)°, $O_2-B_1-C_1-C_2$ 0.9(5)°. Space groups: (a) $P1$; (b) $P2_1/c$.

9−11 (Figure 7). In a comparison of the three halogenated analogues shown in Figure 7, the increase in the offset between two π-stacked dimeric units in moving from the F- to the Cl- and finally to the Br-substituted derivative is easily noted. Specifically, the π-stacked dimers display offsets of 1.40, 6.42, and 8.93 Å, respectively. A closer look reveals that non-covalent halogen−halogen interactions of type I as described by Desiraju[31] (i.e., van der Waals interactions of the dispersion−repulsion type) are present in 4-chloro- and 4-bromophenylboronic acid. In particular, in both cases, on the basis of the observation that the geometrical C−X···X angles are equal to 169.5°, the interaction

is symmetrical. This can be attributed to the need to minimize the repulsion between the two interacting halogen atoms by interfacing the neutral region of their electrostatic potential surface. In addition, a shorter X···X interaction distance is noted for the Cl···Cl contact than for Br···Br (3.30 vs 3.40 Å), with both values being shorter than the sum of the van der Waals radii of the relevant halogen atoms.

Moving on to p-methoxyphenylboronic acid (**7**), a large offset is observed (i.e., 9.32 Å; Figure 8a). In contrast, the thiomethyl analogue **8** is characterized by the placement of the dimeric units both in a parallel and antiparallel manner, the former being
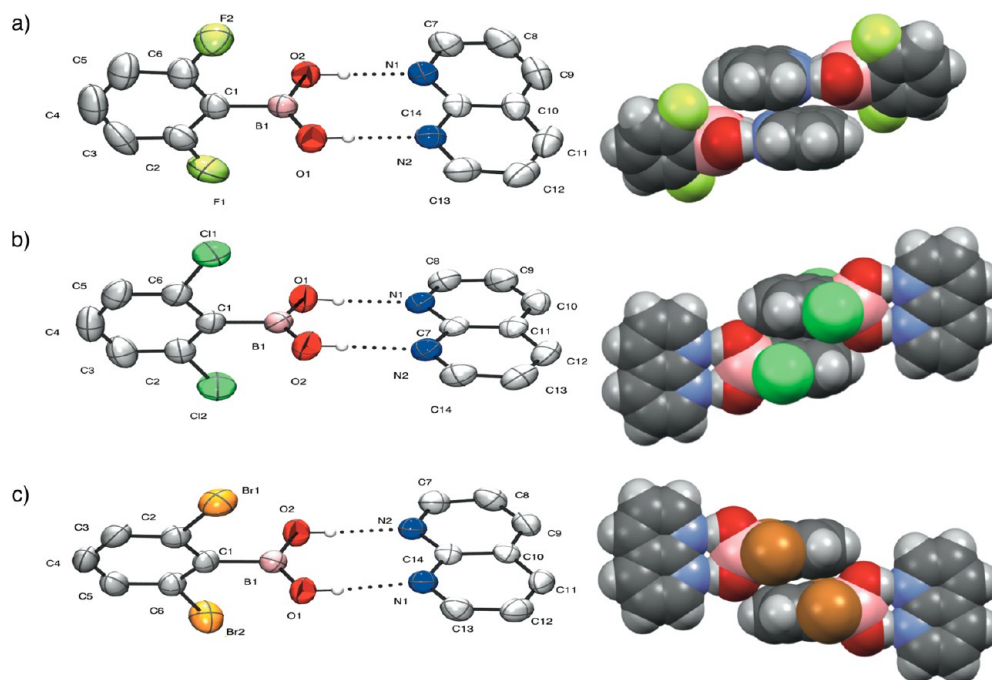
Figure 10. Crystal structures of the dimeric complexes (a) **2·NAP**, (b) **3·NAP**, and (c) **4·NAP**: (left) ORTEP representations drawn at the 30% probability level; (right) space-filling representations. Heteroatom distances for the H-bonds: (a) $N_2 \cdots O_1$ 2.798(2) Å, $N_1 \cdots O_2$ 2.7862(19) Å; (b) $N_2 \cdots O_2$ 2.802(2) Å, $N_1 \cdots O_1$ 2.812(2) Å; (c) $N_1 \cdots O_1$ 2.830(4) Å, $N_2 \cdots O_2$ 2.795(4) Å. Dihedral angles between the aryl and boronic acid groups: (a) $O_1 - B_1 - C_1 - C_2$ 62.7(3)°, $O_2 - B_1 - C_1 - C_6$ 62.4(5)°; (b) $O_1 - B_1 - C_1 - C_2$ 89.4(2)°, $O_2 - B_1 - C_1 - C_6$ 88.7(2)°; (c) $O_1 - B_1 - C_1 - C_2$ 91.2(5)°, $O_2 - B_1 - C_1 - C_6$ 90.3(5)°. Space groups: (a−c) $P2_1/c$.
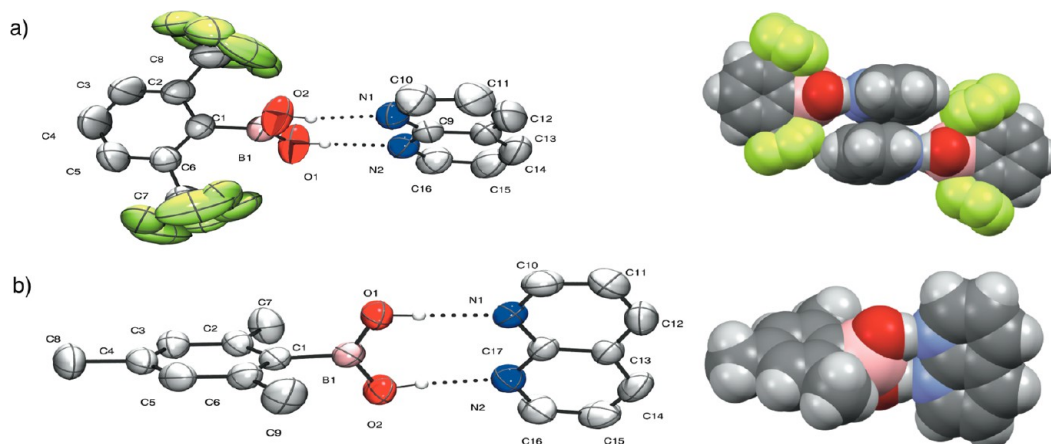

Figure 11. Crystal structures of the dimeric complexes (a) **5·NAP** and (b) **1·NAP**: (left) ORTEP representations drawn at the 30% probability level; (right) space-filling representations. Distances of the H-bonds: (a) $N_2 \cdots O_1$ 2.796(2) Å, $N_1 \cdots O_2$ 2.803(2) Å; (b) $N_1 \cdots O_1$ 2.839(3) Å, $N_2 \cdots O_2$ 2.878(2) Å. Dihedral angles between the aryl and boronic acid groups: (a) $O_1 - B_1 - C_1 - C_6$ 81.3(3)°, $O_2 - B_1 - C_1 - C_2$ 84.4(3)°; (b) $O_1 - B_1 - C_1 - C_6$ 89.6(3)°, $O_1 - B_1 - C_1 - C_6$ 88.1(3)°. Space groups: (a) $P2_1/n$; (b) $P2_1/c$.

driven by weak secondary S···S bonding interactions. Similar behavior is noted for the cocrystals obtained for 3,4,5-trifluorophenylboronic (**13**), which showed local segregation of the hydrogen and fluoride atoms. This drives the formation of a columnar π-stacking arrangement in which the molecules are organized in a parallel fashion.

Similarly, the complexation in the solid state was also investigated with some selected arylboronic acids in the presence of **Phen** as the acceptor. As shown in Figure 9, the molecular arrangements for the complexes of **10** and **13** with **Phen** are very similar to those obtained using **NAP** (Figures 6−8). The *syn*−*syn* conformation is indeed adopted, triggering the interaction with the AA moiety of **Phen** though shorter H-bonding distances

compared with those observed with **NAP** (e.g., boronic acid **13** displays H-bond distances of 2.791 vs 2.820 Å with **Phen** vs **NAP**, respectively). This nicely reflects the solution NMR experiments, which indeed revealed stronger associations when phenylboronic acid derivatives are complexed with the **Phen** moiety.

Dimeric "T-Shaped" Complexes. A pair of H-bonds was also identified in the solid state for the cocrystal obtained between bis-*ortho*-substituted phenylboronic acids and **NAP** (Figure 10). In contrast to the above examples, the presence of the sterically hindering *ortho* substituents triggers the rotation of the boronic acid functional group with respect to the plane of the aryl ring upon formation of the non-covalent complex, resulting in
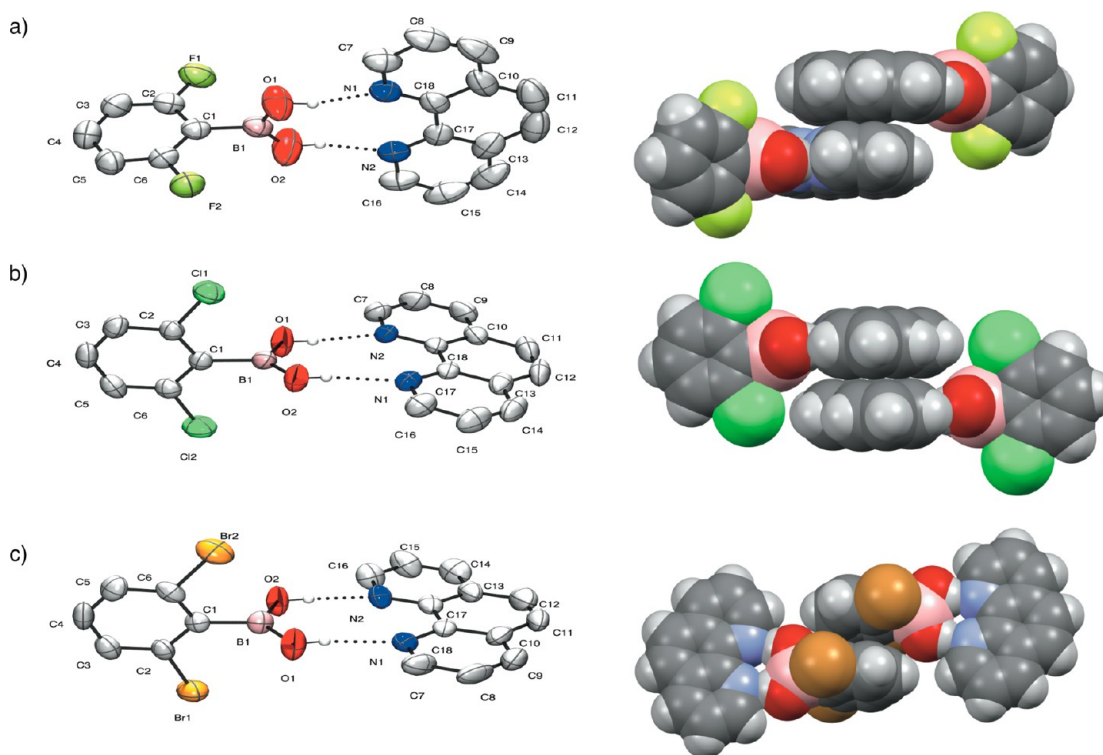
Figure 12. Crystal structures of the dimeric complexes (a) **2·Phen**, (b) **3·Phen**, and (c) **4·Phen**: (left) ORTEP representations drawn at the 30% probability level; (right) space-filling representations. Distances of the H-bonds: (a) $N_1 \cdots O_1$ 2.732(3) Å, $N_2 \cdots O_2$ 2.749(4) Å; (b) $N_2 \cdots O_1$ 2.767(2) Å, $N_1 \cdots O_2$ 2.815(2) Å; (c) $N_1 \cdots O_1$ 2.799(7) Å, $N_2 \cdots O_2$ 2.765(7) Å. Dihedral angles between the aryl and boronic acid groups: (a) $O_1-B_1-C_1-C_2$ 86.8(3)°, $O_2-B_1-C_1-C_6$ 88.6(4)°; (b) $O_1-B_1-C_1-C_6$ 83.7(2)°, $O_2-B_1-C_1-C_2$ 91.1(2)°; (c) $O_1-B_1-C_1-C_6$ 95.6(8)°, $O_2-B_1-C_1-C_2$ 88.9(8)°. Space groups: (a) $P2_1/n$; (b, c) $P2_1/c$.
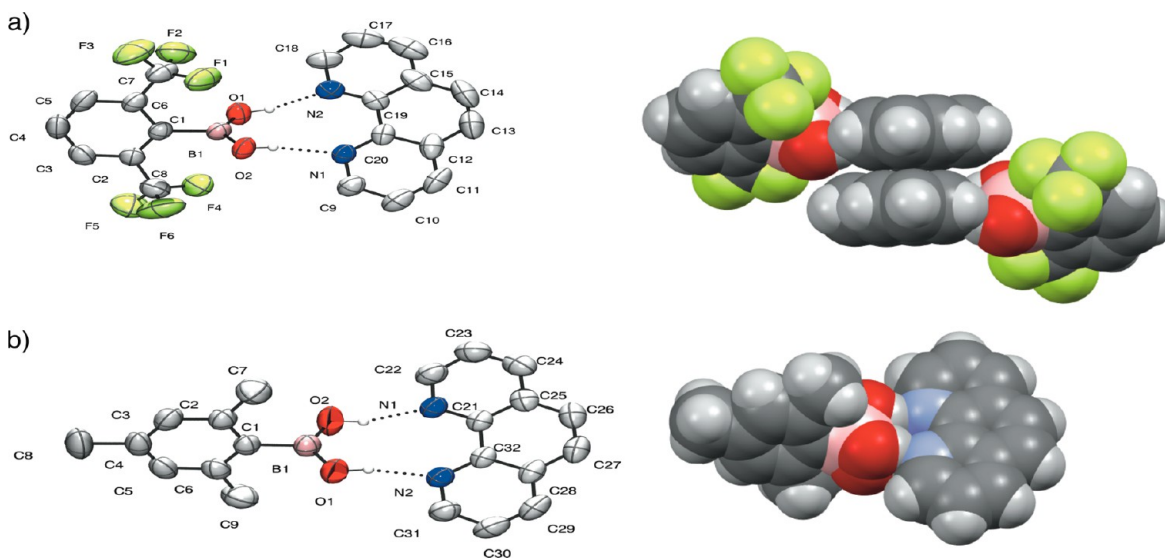

Figure 13. Crystal structures of the dimeric complexes (a) **5·Phen** and (b) **1·Phen**: (left) ORTEP representations drawn at the 30% probability level; (right) space-filling representations. Distances of the H-bonds: (a) $N_2 \cdots O_1$ 2.772(4) Å, $N_1 \cdots O_2$ 2.787(3) Å; (b) $N_2 \cdots O_1$ 2.796(6) Å, $N_1 \cdots O_2$ 2.858(8). Dihedral angles between the aryl and boronic acid groups: (a) $O_1-B_1-C_1-C_6$ 73.1(4)°, $O_2-B_1-C_1-C_2$ 77.8(4)°; (b) $O_1-B_1-C_1-C_6$ 54.3(4)°, $O_2-B_1-C_1-C_2$ 921(4)°. Space groups: (a) $P2_1/c$; (b) $P2/c$.

complexes featuring a "T-shaped" geometry in which the two aromatic scaffolds do not lie in the same plane.

For 2,6-difluorophenylboronic acid (**2**), shorter H-bond distances (2.786 and 2.798 Å; Figure 10a) are observed compared with phenylboronic acid (2.823 and 2.828 Å; Figure 6a). The boronic acid distortion features here an $O_1-B_1-C_1-C_6$ dihedral angle of 62.7°, while the packing of the dimeric units is

characterized by antiparallel stacking of the **NAP** modules of two **2·NAP** complexes through $\pi-\pi$ interactions (3.354 Å). Likewise in the case of 2,6-dichlorophenylboronic acid (**3**) and 2,6-dibromophenylboronic acid (**4**), the torsion angle is almost 90°, induced by the presence of the larger *ortho* substituents (Figure 10b,c). An analogous trend can be observed for 2,6-bis(trifluoromethyl)-phenylboronic (**5**), while for mesitylboronic acid (**1**), the increased
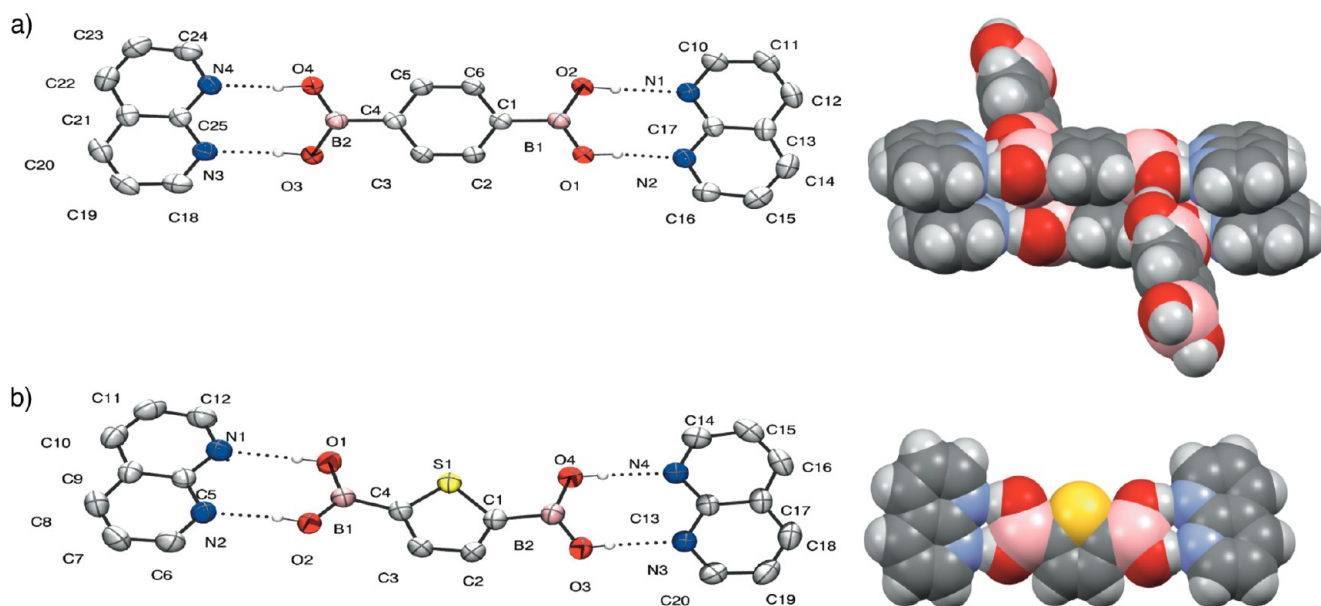
Figure 14. Crystal structures of the trimeric complexes (a) **NAP·17·NAP** and (b) **NAP·18·NAP**: (left) ORTEP representations drawn at the 30% probability level; (right) space-filling representations. Distances of the H-bonds: (a) $N_1 \cdots O_2$ 2.8736(16) Å, $N_2 \cdots O_1$ 2.7420(16) Å, $N_3 \cdots O_3$ 2.8766(16) Å, $N_4 \cdots O_4$ 2.7527(16) Å; (b) $N_1 \cdots O_1$ 2.889(2) Å, $N_2 \cdots O_2$ 2.759(2) Å, $N_3 \cdots O_3$ 2.832(2) Å, $N_4 \cdots O_4$ 2.825(2) Å. Dihedral angles between the aryl and boronic acid groups: (a) $O_1-B_1-C_1-C_2$ 1.3(2)°, $O_2-B_1-C_1-C_6$ 0.7(2)°, $O_3-B_2-C_4-C_3$ 12.7(2)°, $O_4-B_2-C_4-C_5$ 9.4(2)°; (b) $O_1-B_1-C_4-S_1$ 1.8(3)°, $O_2-B_1-C_4-C_3$ 5.8 (3)°, $O_3-B_2-C_1-C_2$ 17.2 (3)°, $O_4-B_2-C_1-S_1$ 15.2 (3)°. Space groups: (a) $P\bar{1}$; (b) $P2_1/c$.

steric hindrance of its substituents impedes the formation of strong π–π interactions between two neighboring complexes (Figure 11). The absence of π–π stacking was also observed when *ortho*-substituted phenylboronic acids were cocrystallized with **Phen** (Figures 12 and 13). The *o*-halogen-disubstituted analogues display smaller H-bond distances with respect to the dimeric complexes with **NAP** (i.e., 2.767 vs 2.802 Å for **3**). Again, this is in agreement with the solution studies, which featured higher association strength with **Phen**. Similarly, the −B(OH)₂ moiety twists perpendicular to the aromatic ring to overcome the steric repulsion with the boronic acid functional group.

Trimeric Complexes and Crystal Self-Sorting. To further investigate the versatility of boronic acids to act as adaptable H-bonding tools in molecular recognition, we used diboronic acids in an attempt to form a 1:2 complexes in which the two DD functionalities (DD–DD) interact with two AA molecules (Figure 14). By evaporation of a 1:1 solution of 1,4-phenylenediboronic acid (**17**) and **NAP**, the planar 1:2 complex **NAP·17·NAP** was successfully obtained. This complex is stabilized by parallel π–π stacks between the aryl and **NAP** moieties with distances of 3.502 and 3.480 Å, respectively (Figure 14a). Additionally, lateral diboronic acid derivatives come into play within the heteromolecular complex by creating a homomolecular branched network by means of lateral OH−H contacts (Figure 14a). The 1:2 complex **NAP·18·NAP**) was also obtained when 2,5-thiophenediboronic acid (**18**) was used (Figure 14b), yet no π–π stacking or additional bridging H-bonding interactions could be observed in the crystal structure.

In addition, monophenylboronic acid derivatives were also explored for the interaction in a 2:1 ratio with a ditopic H-bond acceptor (AA–AA) as a partner. Toward this end, the AA–AA counterpart **TANP** was synthesized according to the literature procedure[21] and then cocrystallized with a variety of aromatic-based boronic acids (i.e., molecules **1**, **3**, **6**, **7**, **10**, **11**, and **16**). The formation of single crystals was achieved by slow evaporation of toluene, and the resulting trimeric complexes were

successfully obtained in all cases, as outlined in Figures 15 and 16. As already observed above, the presence of sterically bulky *ortho* substituents induces the formation of "T-shaped" complexes, as observed for the trimeric complex **3·TANP·3** (Figure 16b). On the other hand, consistent with the dimeric "flat" complexes, also in this case the −B(OH)₂ moiety adopts an in-plane conformation with the aromatic ring with phenyl- and 4-methoxyphenylboronic acid (complexes **6·TANP·6** and **7·TANP·7**, respectively; Figure 15a,d). Notably, shorter H-bond distances, i.e., stronger H-bonding interaction, are observed in going from 2:1 and 1:2 complexes to 1:1 complexes. In fact, taking as examples the complexes including unsubstituted phenylboronic acids (**6** and **17**), the average H-bond distance ranges from 2.825 Å to 2.875 and 2.895 Å for complexes **6·NAP** (1:1), **NAP·17·NAP** (1:2), and **3·TANP·3** (2:1), respectively.

Unexpectedly, when sterically demanding mesitylboronic acid cocrystallizes, it adopts a *syn–anti* conformation, thereby forming a homomolecular dimer (Figure 16a). The **TANP** module here finds its packing motif by entertaining π–π interactions with the aromatic portion of the mesitylboronic acid and additionally interacting through H-bonds with its *anti* B−OH proton (Figure 16a). This is enhanced from the crystal structures of 2,6-dichlorophenyl- and naphthalene-1-boronic acid (Figure 16b,c). In both structures, the 1:2 trimeric complex is noted, but toluene also cocrystallizes. Toluene is partially ordered and occupies 40% of the volume of the crystal in the first case. Specifically, each trimeric unit is separated by a molecule of toluene, both faces of which interact through π–π interactions (3.830 Å) with the ring of the tetraazanaphthacene molecule of each complex. On the other hand, disordered solvent toluene molecules are found in crystals of trimeric complex **16·TANP·16**.

Solid-Phase Self-Sorting Properties. With the goal of examining the self-sorting of two different boronic acids when they are cocrystallized with an equal molar ratio of an acceptor, a solution of **TANP**, **10**, and **11** was allowed to crystallize.
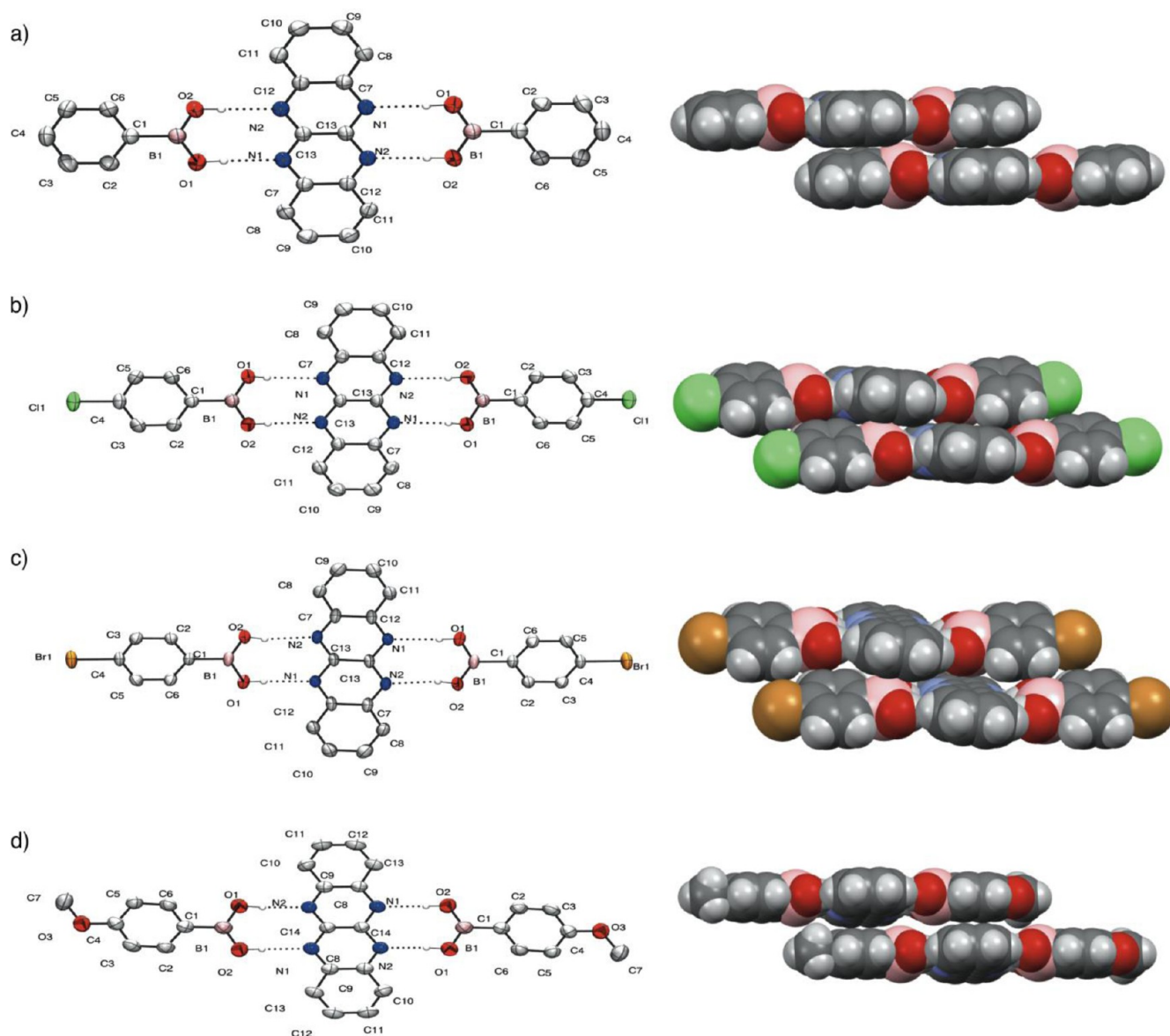
Figure 15. Crystal structures of the trimeric complexes (a) **6·TANP·6**, (b) **10·TANP·10**, (c) **11·TANP·11** and (d) **7·TANP·7**: (left) ORTEP representations drawn at the 30% probability level; (right) space-filling representations. Distances of the H-bonds: (a) $N_2\cdots O_2$ 2.882(4) Å, $N_1\cdots O_1$ 2.908(4) Å; (b) $N_1\cdots O_1$ 2.9031(15) Å, $N_2\cdots O_2$ 2.9261(15) Å; (c) $N_1\cdots O_1$ 2.892(5) Å, $N_2\cdots O_2$ 2.952(5) Å; (d) $N_1\cdots O_2$ 2.921(3) Å, $N_2\cdots O_1$ 2.864(3) Å. Dihedral angles between the aryl and boronic acid groups: (a) $O_2-B_1-C_1-C_6$ 3.9(7)°, $O_1-B_1-C_1-C_2$ 5.0(8)°; (b) $O_2-B_1-C_1-C_2$ 15.5(2)°, $O_1-B_1-C_1-C_6$ 13.9(2)°; (c) $O_2-B_1-C_1-C_2$ 15.4(8)°, $O_1-B_1-C_1-C_6$ 14.9(8)°; (d) $O_2-B_1-C_1-C_2$ 3.6(4)°, $O_1-B_1-C_1-C_6$ 4.0(4)°. Space groups: (a–c) $P\bar{1}$; (d) $P2_1/n$.

As one can observe from the optical microscopy images (Figure 17), crystals with similar appearance were obtained. X-ray diffraction analysis revealed that the crystal lattice contains 40% **11** and 60% **10**. Because of the similarity between the electron densities of the Cl and Br atoms, we could not unequivocally establish whether each trimeric unit contains both boronic acids or only one. In terms of H-bonding distances, $N_1\cdots O_2$ distances similar to those described in Figure 16 were measured.

However, when the same cocrystallization experiments were repeated with one of the two halogenated analogues replaced with naphthalene-1-boronic acid (**16**), different crystals were obtained (Figure 18c). Comparing these crystals to those obtained from separate crystallization experiments (see the crystals in Figure 18a,b), one can easily conclude that the forming trimeric **X·TANP·X** complexes undergo self-sorting, leading to two types

of crystals, each containing a unique 2:1 complex: **16·TANP·16** and **11·TANP·11** (Figure 18c). Single-crystal X-ray diffraction analysis of the obtained crystal mixture revealed that crystals containing both boronic acids were never detected in any of the analyzed samples. This means that the supramolecular complexes **16·TANP·16** and **11·TANP·11** are formed and spontaneously self-sorted into two crystalline phases.

Polymeric Complexes (AA·DD)$_n$: Toward Supramolecular Materials. The ultimate extension of our studies was the engineering of an expanded version of these di- or trimeric non-covalent complex systems and hence the formation of a supramolecular network. As a result, the goal was to achieve the formation of crystals containing both ditopic molecular modules **17** and **TANP**. The major experimental difficulty that arose was either the poor solubility of the boronic acid in nonpolar solvents or that of the acceptor in polar solvents. However, through
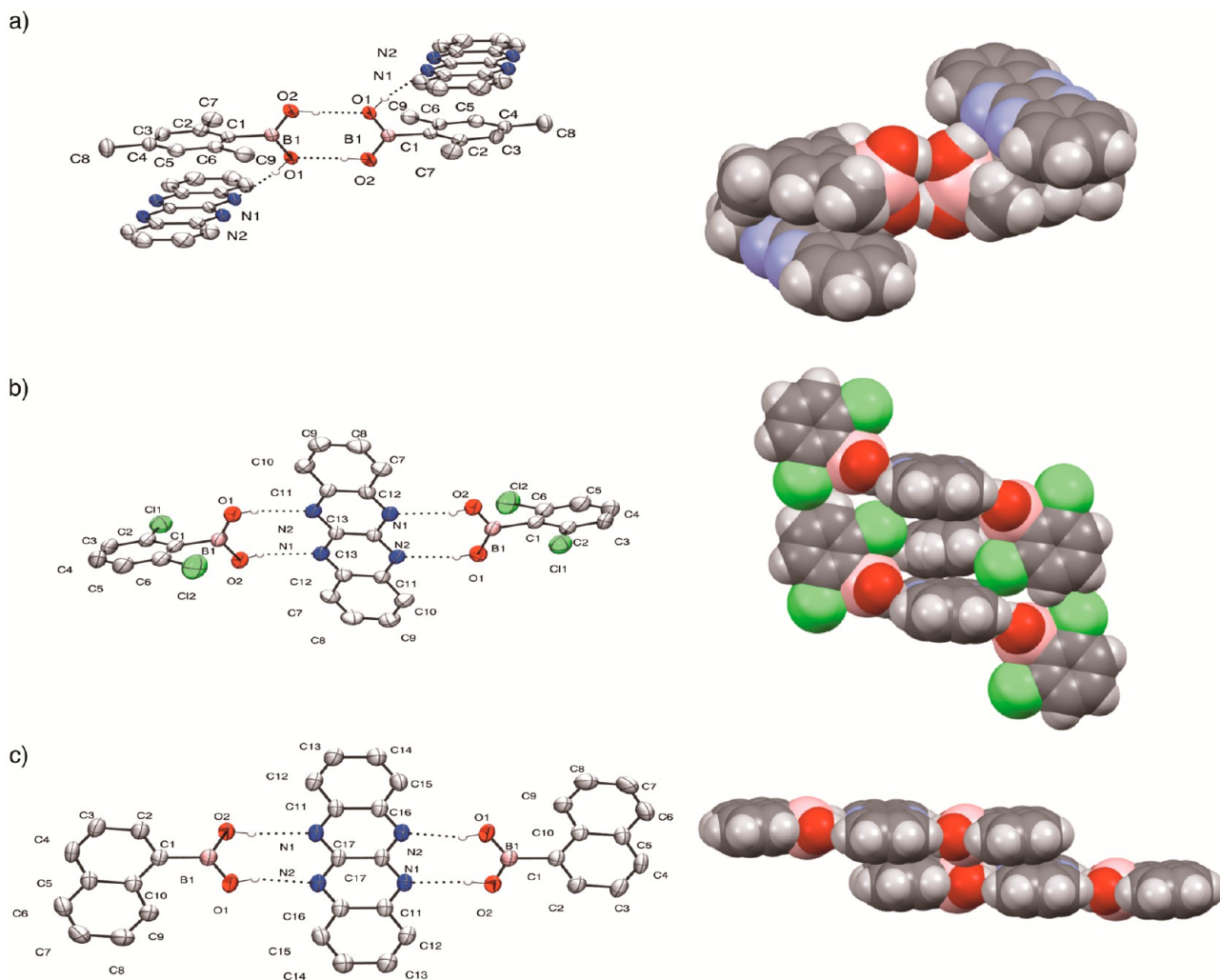
Figure 16. Crystal structures of the trimeric complexes (a) **1·TANP·1**, (b) **3·TANP·3**, and (c) **16·TANP·16**: (left) ORTEP representations drawn at the 30% probability level; (right) space-filling representations. Distances of the H-bonds: (a) $N_2 \cdots O_1$ 2.865(4) Å, $N_1 \cdots O_2$ 2.914(4) Å; (b) $O_1 \cdots O_2$ 2.831(3) Å, $N_1 \cdots O_1$ 2.945(2) Å; (c) $N_2 \cdots O_1$ 2.876(2) Å, $N_1 \cdots O_2$ 2.937(2) Å. Dihedral angles between the aryl and boronic acid groups: (a) $O_2-B_1-C_1-C_2$ 91.7(4)°, $O_1-B_1-C_1-C_6$ 90.8(4)°; (b) $O_2-B_1-C_1-C_6$ 92.6(2)°, $O_1-B_1-C_1-C_2$ 91.0(2)°; (c) $O_2-B_1-C_1-C_2$ 3.1(3)°, $O_1-B_1-C_1-C_6$ 2.8(3)°. Space groups: (a) $P2_1/n$; (b, c) $P\overline{1}$.

Figure 17. Optical microscopy images of the single crystals obtained from the trimeric complexes of **TANP** with (a) 4-chlorophenylboronic acid (**10**), (b) 4-bromophenylboronic acid (**11**), and (c) an equimolar solution of **10** and **11**.

screening of a large variety of solvents and temperatures, we noticed that both molecules are soluble in water under reflux conditions and that upon cooling to different temperatures for a period of 24 h the mixture gave rise to different types of crystals. For instance, when the solution was cooled to 25 °C, an orange powdery precipitate was noted (Figure 19a), whereas at 35 °C only needlelike deep-red crystals of **TANP** (confirmed by X-ray analysis) were obtained (Figure 19c). However, at a cooling temperature of 30 °C, the solid phase could be amended to orange flaky crystals (Figure 19b), suggesting the presence of both molecules in each crystal. This was further confirmed by

single-crystal X-ray diffraction analysis, which revealed the formation of polymeric-like ribbons (**17·TANP**)$_n$, in which the single molecular components are held together by double DD·AA H-bonds. Within the polymeric assembly, the $N_1 \cdots O_1$ and $N_2 \cdots O_2$ distances are equal to 2.863 and 2.876 Å, with the boronic acid functionality being coplanar with the **TANP** aromatic structure (Figure 20a). The H-bonded ribbons are supramolecularly arranged in striped patterned sheets (Figure 20b) that are organized in a multilayered, graphite-like fashion displaying an average interplanar distance of 3.366 Å (Figure 20c). At the molecular level, the sheets are arranged in multilayers
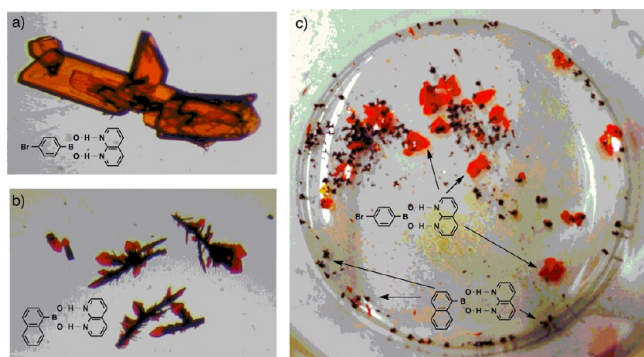
Figure 18. Optical microscopy images of the single crystals obtained from the trimeric complexes of **TANP** with (a) 4-bromophenylboronic acid (**11**), (b) naphthalene-1-boronic acid (**16**), and (c) an equimolar solution of **11** and **16**.

through π−π stacking interactions, where each boronic acid aryl ring is π-sandwiched between two acceptor **TANP** molecules belonging to the nearest supramolecular sheets. As observed by optical microscopy (Figure 19b) and scanning electron microscopy (SEM) (Figure 19d−f), the sheetlike arrangement at the molecular level is expressed at longer length scales by the formation of crystals with a flaky morphology.

CONCLUSIONS

We have demonstrated the feasibility of using arylboronic acids to form H-bonded DD·AA-type complexes with suitable acceptor partners. Most importantly, the determination of K_a values through solution-state binding studies of such complexes are reported here for the first time. In particular, K_a values ranging between 369 and 6900 M^{-1} were noted for *ortho*-substituted boronic acid analogues; the values are strongly dependent on the substituents and the complexation partner. **Phen** provided stronger complexes than **NAP**, possibly caused by stronger

secondary electrostatic N···H interactions, as seen by analysis of the electronic surface potential. Additional parameters taken under consideration were the homodimer formation constant (K_d), which proved to be negligible; the boroxine formation constant (K_{borox}), which was mainly observed when non-*ortho*-substituted analogues were used; and hydroxyboronate ion formation (K_i), for which direct evidence of its effect could not be observed. Binding studies in the solid state led to the formation of both dimeric 1:1 and trimeric 1:2 and 2:1 complexes. Extensive analysis of these crystal structures revealed that "flat" complexes are the result of non-*ortho*-substituted boronic acids, in contrast with the "T-shaped" complexes arising from more sterically demanding *ortho*-substituted analogues. This showcases the unique ability of the boronic acids to self-adapt while retaining their recognition property. The existence of π−π interactions in both the dimeric and trimeric complexes is affected by the presence and bulkiness of the *ortho* substituents, a parameter that influences the distance of the H-bonds as well. The results obtained in solution are in accordance with the solid-state results, since shorter H-bond distances are noted in the cases were **Phen** is the complexation partner. To the best of our knowledge, this paper for the first time describes a supramolecular H-bonded polymer involving a boronic acid, which was successfully constructed through the donor−acceptor interaction between ditopic 1,4-phenylenediboronic acid and **TANP**. The resulting highly ordered monodimensional polymeric material features infinite ribbonlike arrays running parallel, as observed by SEM. We believe that this study further strengthens the potential of the boronic acid functional group as a potent building block in supramolecular chemistry, not only as dynamic reactive species for dynamic covalent chemistries but also through H-bond recognition. Future challenges would be to apply this principle in the considerate choice of complexation partners to construct functional and operative supramolecular architectures both in the solid state and in solution, which could feature structural and
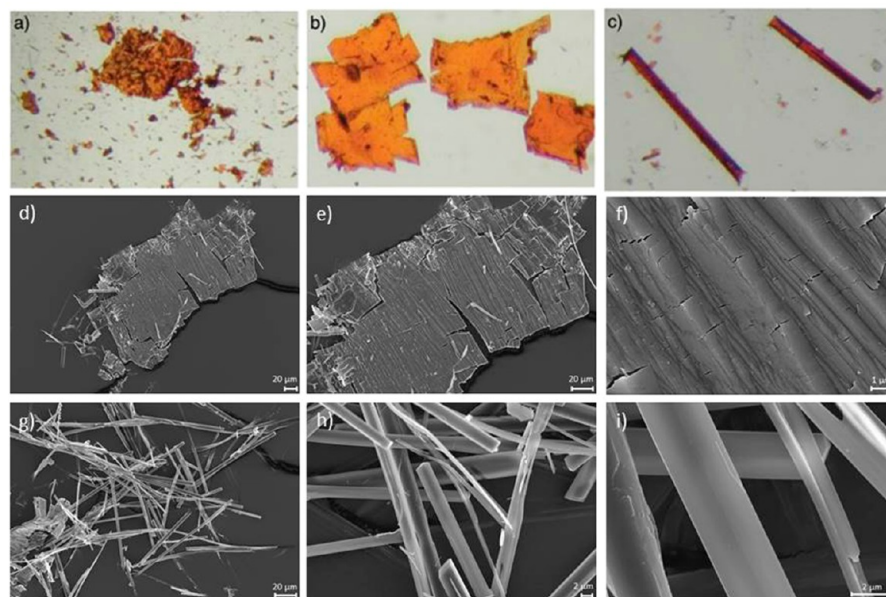

Figure 19. (a−c) Optical microscopy images of the crystals obtained when an equimolar solution of 1,4-phenylenediboronic acid (**17**) and **TANP** were heated at 100 °C and then cooled to (a) 25 °C, (b) 30 °C, or (c) 35 °C. (d−f) SEM images of a single crystal of the heteromolecular supramolecular polymer displaying an anisotropic lamellar-type organization at different magnifications: (d) 517×, (e) 1000×, and (f) 20000×. (g−i) SEM images of single crystals of **TANP** obtained by cooling to 35 °C at different magnifications: (g) 1000×, (h) 5000×, and (i) 20000×.
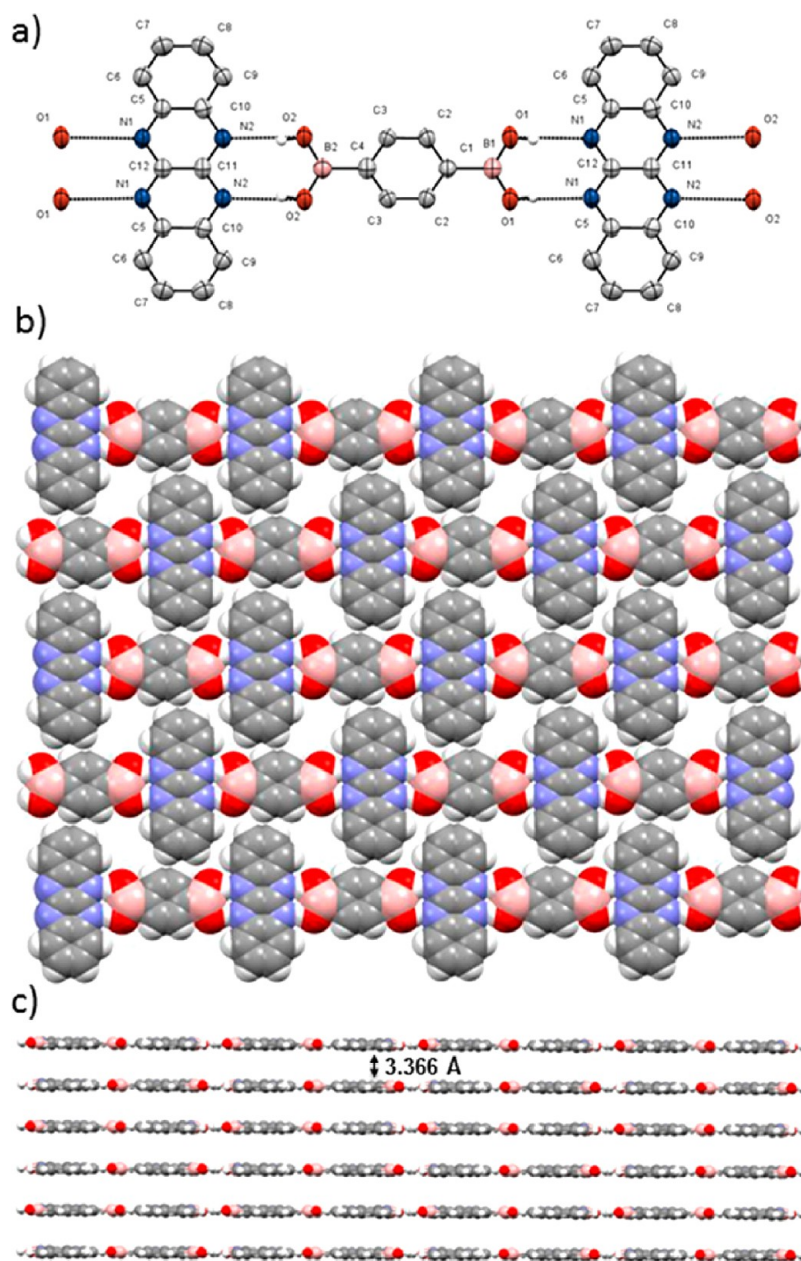
Figure 20. Crystal structure of the heteromolecular supramolecular polymer ($\mathbf{17 \cdot TANP}$)$_n$. (a) ORTEP representation of the crystal structure (drawn at the 30% probability level). (b) Space-filling representation of the in-plane zipped organization of the supramolecular polymer. (c) Lamellar-like arrangement displaying an interplanar distance of 3.36 Å (calculated between two planes averaging 600 atoms). Heteroatom distances of the H-bonds: $N_1 \cdots O_1$ 2.863(3) Å, $N_2 \cdots O_2$ 2.876(3) Å. Dihedral angles between the aryl and boronic acid groups: (a) $O_2-B_1-C_4-C_3$ 3.27(15)°, $O_1-B_1-C_1-C_2$ 1.83(15)°. Space group: $P2/c$.

physical properties that would be useful in areas such as organic materials for printed electronics and organocatalysis.

■ ASSOCIATED CONTENT

Ⓢ Supporting Information

The Supporting Information is available free of charge on the ACS Publications website at DOI: 10.1021/jacs.6b11362.

Synthetic protocols, spectroscopic characterizations, titration experiments, theoretical details, and X-ray parameters (PDF)

Crystallographic data for **6·NAP** (CIF)

Crystallographic data for **2·NAP** (CIF)

Crystallographic data for **3·Phen** (CIF)

Crystallographic data for **3·NAP** (CIF)

Crystallographic data for **2·Phen** (CIF)

Crystallographic data for **4·NAP** (CIF)

Crystallographic data for **4·Phen** (CIF)

Crystallographic data for **1·NAP** (CIF)

Crystallographic data for **9·NAP** (CIF)

Crystallographic data for **10·NAP** (CIF)

Crystallographic data for **10·Phen** (CIF)

Crystallographic data for **11·NAP** (CIF)

Crystallographic data for **7·NAP** (CIF)

Crystallographic data for **8·NAP** (CIF)

Crystallographic data for **12·NAP** (CIF)

Crystallographic data for **13·NAP** (CIF)

Crystallographic data for **13·Phen** (CIF)

■ AUTHOR INFORMATION

Corresponding Author
*bonifazid@cardiff.ac.uk

ORCID ⓘ
Davide Bonifazi: 0000-0001-5717-0121

Notes
The authors declare no competing financial interest.

■ ACKNOWLEDGMENTS

■ REFERENCES

(1) *Boronic Acids: Preparation and Applications in Organic Synthesis and Medicine*; Hall, D. G., Ed.; Wiley-VCH: Weinheim, Germany, 2005.
(2) (a) James, T. D. *Beilstein J. Org. Chem.* **2016**, *12*, 391. (b) Nishiyabu, R.; Kubo, Y.; James, T. D.; Fossey, J. S. *Chem. Commun.* **2011**, *47*, 1124. (c) Kubo, Y.; Nishiyabu, R.; James, T. D. *Chem. Commun.* **2015**, *51*, 2005. (d) Fujita, N.; Shinkai, S.; James, T. D. *Chem. - Asian J.* **2008**, *3*, 1076. (e) Corbett, P. T.; Leclaire, J.; Vial, L.; West, K. R.; Wietor, J. L.; Sanders, J. K. M.; Otto, S. *Chem. Rev.* **2006**, *106*, 3652.
(3) For some topical papers, see: (a) Nishiyabu, R.; Kubo, Y.; James, T. D.; Fossey, J. S. *Chem. Commun.* **2011**, *47*, 1106. (b) Brooks, W. L. A.; Sumerlin, B. S. *Chem. Rev.* **2016**, *116*, 1375. (c) Sun, X.; James, T. D. *Chem. Rev.* **2015**, *115*, 8001. (d) Wu, J.; Kwon, B.; Liu, W.; Anslyn, E. V.; Wang, P.; Kim, J. S. *Chem. Rev.* **2015**, *115*, 7893. (e) You, L.; Zha, D.; Anslyn, E. V. *Chem. Rev.* **2015**, *115*, 7840. (f) Li, M.; Zhu, W.; Marken, F.; James, T. D. *Chem. Commun.* **2015**, *51*, 14562. For selected recent papers in the field, see: (g) Oesch, D.; Luedtke, N. W. *Chem. Commun.* **2015**, *51*, 12641. (h) Zhong, Z.; Anslyn, E. V. *J. Am. Chem. Soc.* **2002**, *124*, 9014. (i) Zhu, L.; Anslyn, E. V. *J. Am. Chem. Soc.* **2004**, *126*, 3676. (j) Zhu, L.; Zhong, Z.; Anslyn, E. V. *J. Am. Chem. Soc.* **2005**, *127*, 4260. (k) Sun, X.; Zhai, W.; Fossey, J. S.; James, T. D. *Chem. Commun.* **2016**, *52*, 3456. (l) Sun, X.; Xu, S.-Y.; Flower, S. E.; Fossey, J. S.; Qian, X.; James, T. D. *Chem. Commun.* **2013**, *49*, 8311.

(4) (a) Aelvoet, K.; Batsanov, A. S.; Blatch, A. J.; Grosjean, C.; Patrick, L. G. F.; Smethurst, C. A.; Whiting, A. *Angew. Chem., Int. Ed.* **2008**, *47*, 768. (b) Georgiou, I.; Ilyashenko, G.; Whiting, A. *Acc. Chem. Res.* **2009**, *42*, 756.
(5) For some topical reviews, see: (a) Rowan, S. J.; Cantrill, S. J.; Cousins, G. R. L.; Sanders, J. K. M.; Stoddart, J. F. *Angew. Chem., Int. Ed.* **2002**, *41*, 898. (b) Lehn, J. M. *Chem. Soc. Rev.* **2007**, *36*, 151. (c) Jin, Y.; Yu, C.; Denman, R. J.; Zhang, W. *Chem. Soc. Rev.* **2013**, *42*, 6634. (d) Wilson, A.; Gasparini, G.; Matile, S. *Chem. Soc. Rev.* **2014**, *43*, 1948. For selected recent papers in the field, see: (e) Rodriguez-Docampo, Z.; Otto, S. *Chem. Commun.* **2008**, 5301. (f) Sarma, R. J.; Otto, S.; Nitschke, J. R. *Chem. - Eur. J.* **2007**, *13*, 9542. (g) Lascano, S.; Zhang, K.-D.; Wehlauch, R.; Gademann, K.; Sakai, N.; Matile, S. *Chem. Sci.* **2016**, *7*, 4720. (h) Zhang, K.-D.; Sakai, N.; Matile, S. *Org. Biomol. Chem.* **2015**, *13*, 8687. (i) Zhang, K.-D.; Matile, S. *Angew. Chem., Int. Ed.* **2015**, *54*, 8980. (j) Fin, A.; Petkova, I.; Doval, D. A.; Sakai, N.; Vauthey, E.; Matile, S. *Org. Biomol. Chem.* **2011**, *9*, 8246. (k) Rocard, L.; Berezin, A.; De Leo, F.; Bonifazi, D. *Angew. Chem., Int. Ed.* **2015**, *54*, 15739. (l) Nishiyabu, R.; Teraoka, S.; Matsushima, Y.; Kubo, Y. *ChemPlusChem* **2012**, *77*, 201. (m) Seifert, H. M.; Trejo, K. R.; Anslyn, E. V. *J. Am. Chem. Soc.* **2016**, *138*, 10916. (n) Christinat, N.; Croisier, E.; Scopelliti, R.; Cascella, M.; Röthlisberger, U.; Severin, K. *Eur. J. Inorg. Chem.* **2007**, *2007*, 5177. (o) Colson, J. W.; Woll, A. R.; Mukherjee, A.; Levendorf, M. P.; Spitler, E. L.; Shields, V. B.; Spencer, M. G.; Park, J.; Dichtel, W. R. *Science* **2011**, *332*, 228.
(6) (a) Iwasawa, N.; Takahagi, H. *J. Am. Chem. Soc.* **2007**, *129*, 7754. (b) Kataoka, K.; Okuyama, S.; Minami, T.; James, T. D.; Kubo, Y. *Chem. Commun.* **2009**, 1682. (c) Kataoka, K.; James, T. D.; Kubo, Y. *J. Am. Chem. Soc.* **2007**, *129*, 15126. (d) Takahagi, H.; Fujibe, S.; Iwasawa, N. *Chem. - Eur. J.* **2009**, *15*, 13327.
(7) (a) Iovine, P. M.; Gyselbrecht, C. R.; Perttu, E. K.; Klick, C.; Neuwelt, A.; Loera, J.; Di Pasquale, A. G.; Rheingold, A. L.; Kua, J. *Dalton Trans.* **2008**, 3791. (b) Perttu, E. K.; Arnold, M.; Iovine, P. M. *Tetrahedron Lett.* **2005**, *46*, 8753. (c) Côté, A. P.; Benin, A. I.; Ockwig, N. W.; O'Keeffe, M.; Matzger, A. J.; Yaghi, O. M. *Science* **2005**, *310*, 1166. (d) Li, Y.; Ding, J.; Day, M.; Tao, Y.; Lu, J.; D'Iorio, M. *Chem. Mater.* **2003**, *15*, 4936.
(8) (a) Kameta, N.; Hiratani, K. *Tetrahedron Lett.* **2006**, *47*, 4947. (b) Kameta, N.; Hiratani, K. *Chem. Commun.* **2005**, 725. (c) Danjo, H.; Hirata, K.; Yoshigai, S.; Azumaya, I.; Yamaguchi, K. *J. Am. Chem. Soc.* **2009**, *131*, 1638.
(9) Campos-Gaxiola, J. J.; Vega-Paz, A.; Román-Bravo, P.; Höpfl, H.; Sánchez-Vázquez, M. *Cryst. Growth Des.* **2010**, *10*, 3182.
(10) (a) Rettig, S. J.; Trotter, J. *Can. J. Chem.* **1977**, *55*, 3071. (b) Cyrański, M. K.; Jezierska, A.; Klimentowska, P.; Panek, J. J.; Sporzyński, A. *J. Phys. Org. Chem.* **2008**, *21*, 472.
(11) (a) Fournier, J. H.; Maris, T.; Wuest, J. D.; Guo, W.; Galoppini, E. *J. Am. Chem. Soc.* **2003**, *125*, 1002. (b) Wuest, J. D. *Chem. Commun.* **2005**, 5830. (c) Maly, K. E.; Malek, N.; Fournier, J. H.; Rodríguez-Cuamatzi, P.; Maris, T.; Wuest, J. D. *Pure Appl. Chem.* **2006**, *78*, 1305.
(12) (a) Adamczyk-Woźniak, A.; Cyrański, M. K.; Dąbrowska, A.; Gierczyk, B.; Klimentowska, P.; Schroeder, G.; Zubrowska, A.; Sporzyński, A. *J. Mol. Struct.* **2009**, *920*, 430. (b) Cyrański, M. K.; Klimentowska, P.; Rydzewska, A.; Serwatowski, J.; Sporzyński, A.; Stępień, D. K. *CrystEngComm* **2012**, *14*, 6282. (c) Adamczyk-Woźniak, A.; Brzózka, Z.; Dąbrowski, M.; Madura, I. D.; Scheidsbach, R.; Tomecka, E.; Żukowski, K.; Sporzyński, A. *J. Mol. Struct.* **2013**, *1035*, 190. (d) TalwelkarShimpi, M.; Öberg, S.; Giri, L.; Pedireddi, V. R. *RSC Adv.* **2016**, *6*, 43060.
(13) (a) Scouten, W. H.; Liu, X. C.; Khangin, N.; Mullica, D. F.; Sappenfield, E. L. *J. Chem. Crystallogr.* **1994**, *24*, 621. (b) Zhao, J.; Davidson, M. G.; Mahon, M. F.; Kociok-Köhn, G.; James, T. D. *J. Am. Chem. Soc.* **2004**, *126*, 16179. (c) Coghlan, S. W.; Giles, R. L.; Howard, J. A. K.; Patrick, L. G. F.; Probert, M. R.; Smith, G. E.; Whiting, A. *J. Organomet. Chem.* **2005**, *690*, 4784. (d) Yoshino, J.; Kano, N.; Kawashima, T. *Tetrahedron* **2008**, *64*, 7774. (e) Adamczyk-Woźniak, A.; Brzózka, Z.; Cyrański, M. K.; Filipowicz-Szymańska, A.; Klimentowska, P.; Żubrowska, A.; Żukowski, K.; Sporzyński, A. *Appl. Organomet. Chem.* **2008**, *22*, 427. (f) Adamczyk-Woźniak, A.; Madura, I.;

Pawełko, A.; Sporzyński, A.; Żubrowska, A.; Żyła, J. *Cent. Eur. J. Chem.* **2011**, *9*, 199. (g) Adamczyk-Woźniak, A.; Fratila, R. M.; Madura, I. D.; Pawełko, A.; Sporzyński, A.; Tumanowicz, M.; Velders, A. H.; Żyła, J. *Tetrahedron Lett.* **2011**, *52*, 6639. (h) Adamczyk-Woźniak, A.; Cyrański, M. K.; Frączak, B. T.; Lewandowska, A.; Madura, I. D.; Sporzyński, A. *Tetrahedron* **2012**, *68*, 3761.

(14) (a) Luliński, S.; Madura, I.; Serwatowski, J.; Szatyłowicz, H.; Zachara, J. *New J. Chem.* **2007**, *31*, 144. (b) Rodríguez-Cuamatzi, P.; Tlahuext, H.; Höpfl, H. *Acta Crystallogr., Sect. E: Struct. Rep. Online* **2009**, *65*, o44. (c) Durka, K.; Gontarczyk, K.; Kliś, T.; Serwatowski, J.; Woźniak, K. *Appl. Organomet. Chem.* **2012**, *26*, 287. (d) Durka, K.; Jarzembska, K. N.; Kamiński, R.; Luliński, S.; Serwatowski, J.; Woźniak, K. *Cryst. Growth Des.* **2012**, *12*, 3720. (e) Madura, I. D.; Czerwińska, K.; Sołdańska, D. *Cryst. Growth Des.* **2014**, *14*, 5912.

(15) Sakakura, A.; Yamashita, R.; Ohkubo, T.; Akakura, M.; Ishihara, K. *Aust. J. Chem.* **2011**, *64*, 1458.

(16) (a) Regueiro-Figueroa, M.; Djanashvili, K.; Esteban-Gómez, D.; de Blas, A.; Platas-Iglesias, C.; Rodríguez-Blas, T. *Eur. J. Org. Chem.* **2010**, *2010*, 3237. (b) SeethaLekshmi, N.; Pedireddi, V. R. *Cryst. Growth Des.* **2007**, *7*, 944.

(17) (a) Rodríguez-Cuamatzi, P.; Arillo-Flores, O. I.; Bernal-Uruchurtu, M. I.; Höpfl, H. *Cryst. Growth Des.* **2005**, *5*, 167. (b) Rogowska, P.; Cyrański, M. K.; Sporzyński, A.; Ciesielski, A. *Tetrahedron Lett.* **2006**, *47*, 1389. (c) Aakeröy, C. B.; Desper, J.; Levin, B. *CrystEngComm* **2005**, *7*, 102. (d) SeethaLekshmi, S.; Varughese, S.; Giri, L.; Pedireddi, V. R. *Cryst. Growth Des.* **2014**, *14*, 4143. (e) Hernández-Paredes, J.; Olvera-Tapia, A. L.; Arenas-García, J. I.; Höpfl, H.; Morales-Rojas, H.; Herrera-Ruiz, D.; Gonzaga-Morales, A. I.; Rodríguez-Fragoso, L. *CrystEngComm* **2015**, *17*, 5166. (f) Pedireddi, V. R.; SeethaLekshmi, N. *Tetrahedron Lett.* **2004**, *45*, 1903. (g) Rodríguez-Cuamatzi, P.; Luna-García, R.; Torres-Huerta, A.; Bernal-Uruchurtu, M. I.; Barba, V.; Höpfl, H. *Cryst. Growth Des.* **2009**, *9*, 1575. (h) Talwelkar, M.; Pedireddi, V. R. *Tetrahedron Lett.* **2010**, *51*, 6901. (i) Varughese, S.; Azim, Y.; Desiraju, G. R. *J. Pharm. Sci.* **2010**, *99*, 3743. (j) Varughese, S.; Sinha, S. B.; Desiraju, G. R. *Sci. China: Chem.* **2011**, *54*, 1909.

(18) Wang, J.; Zhang, Y. *ACS Catal.* **2016**, *6*, 4871.

(19) (a) Echavarren, A.; Galan, A.; Lehn, J. M.; de Mendoza, J. *J. Am. Chem. Soc.* **1989**, *111*, 4994. (b) Segura, M.; Alcazar, V.; Prados, P.; de Mendoza, J. *Tetrahedron* **1997**, *53*, 13119.

(20) (a) Jorgensen, W. L.; Pranata, J. *J. Am. Chem. Soc.* **1990**, *112*, 2008. (b) Kawahara, S.; Uchimaru, T. *J. Comput. Chem., Jpn.* **2004**, *3*, 41. (c) Djurdjevic, S.; Leigh, D. A.; McNab, H.; Parsons, S.; Teobaldi, G.; Zerbetto, F. *J. Am. Chem. Soc.* **2007**, *129*, 476.

(21) (a) Isoda, K.; Nakamura, M.; Tatenuma, T.; Ogata, H.; Sugaya, T.; Tadokoro, M. *Chem. Lett.* **2012**, *41*, 937. (b) Rashkin, M. J.; Hughes, R. M.; Calloway, N. T.; Waters, M. L. *J. Am. Chem. Soc.* **2004**, *126*, 13320.

(22) (a) Sijbesma, R. P.; Beijer, F. H.; Brunsveld, L.; Folmer, B. J. B.; Hirschberg, J. H. K. K.; Lange, R. F. M.; Lowe, J. K. L.; Meijer, E. W. *Science* **1997**, *278*, 1601. (b) Brunsveld, L.; Folmer, B. J. B.; Meijer, E. W.; Sijbesma, R. P. *Chem. Rev.* **2001**, *101*, 4071. (c) de Greef, T. F. A.; Meijer, E. W. *Nature* **2008**, *453*, 171. (d) de Greef, T. F. A.; Smulders, M. M. J.; Wolffs, M.; Schenning, A. P. H. J.; Sijbesma, R. P.; Meijer, E. W. *Chem. Rev.* **2009**, *109*, 5687. (e) Aida, T.; Meijer, E. W.; Stupp, S. I. *Science* **2012**, *335*, 813.

(23) Larkin, J. D.; Bhat, K. L.; Markham, G. D.; Brooks, B. R.; Schaefer, H. F., III; Bock, C. W. *J. Phys. Chem. A* **2006**, *110*, 10633.

(24) (a) Tokunaga, Y.; Ueno, H.; Shimomura, Y. *Heterocycles* **2007**, *74*, 219. (b) Tokunaga, Y.; Ueno, H.; Shimomura, Y.; Seo, T. *Heterocycles* **2002**, *57*, 787. (c) Spitler, E. L.; Giovino, M. R.; White, S. L.; Dichtel, W. R. *Chem. Sci.* **2011**, *2*, 1588.

(25) (a) Beijer, F. H.; Sijbesma, R. P.; Vekemans, J. A. J. M.; Meijer, E. W.; Kooijman, H.; Spek, A. L. *J. Org. Chem.* **1996**, *61*, 6371. (b) Đorđević, L.; Marangoni, T.; Miletić, T.; Rubio-Magnieto, J.; Mohanraj, J.; Amenitsch, H.; Pasini, D.; Liaros, N.; Couris, S.; Armaroli, N.; Surin, M.; Bonifazi, D. *J. Am. Chem. Soc.* **2015**, *137*, 8150.

(26) (a) Lorand, J. P.; Edwards, J. O. *J. Org. Chem.* **1959**, *24*, 769. (b) Pizer, R.; Tihal, C. *Inorg. Chem.* **1992**, *31*, 3243. (c) Watanabe, E.; Miyamoto, C.; Tanaka, A.; Iizuka, K.; Iwatsuki, S.; Inamo, M.; Takagi, H. D.; Ishihara, K. *Dalton Trans.* **2013**, *42*, 8446. (d) Okamoto, T.; Tanaka, A.; Watanabe, E.; Miyazaki, T.; Sugaya, T.; Iwatsuki, S.; Inamo, M.; Takagi, H. D.; Odani, A.; Ishihara, K. *Eur. J. Inorg. Chem.* **2014**, *2014*, 2389. (e) Furikado, Y.; Nagahata, T.; Okamoto, T.; Sugaya, T.; Iwatsuki, S.; Inamo, M.; Takagi, H. D.; Odani, A.; Ishihara, K. *Chem. - Eur. J.* **2014**, *20*, 13194.

(27) (a) Tomsho, J. W.; Benkovic, S. J. *J. Org. Chem.* **2012**, *77*, 2098. (b) Ni, W.; Fang, H.; Springsteen, G.; Wang, B. *J. Org. Chem.* **2004**, *69*, 1999. (c) Fan, X.; Freslon, S.; Daiguebonne, C.; Le Pollès, L.; Calvez, G.; Bernot, K.; Yi, X.; Huang, G.; Guillou, O. *Inorg. Chem.* **2015**, *54*, 5534.

(28) Thordarson, P. *Chem. Soc. Rev.* **2011**, *40*, 1305.

(29) (a) Zimmerman, S. C.; Murray, T. J. *Tetrahedron Lett.* **1994**, *35*, 4077. (b) Sartorius, J.; Schneider, H. J. *Chem. - Eur. J.* **1996**, *2*, 1446. (c) Tamashiro, B. T.; Cedano, M. R.; Pham, A. T.; Smith, D. K. *J. Phys. Chem. C* **2015**, *119*, 12865.

(30) Cook, J. L.; Hunter, C. A.; Low, C. M. R.; Perez-Velasco, A.; Vinter, J. G. *Angew. Chem., Int. Ed.* **2007**, *46*, 3706.

(31) (a) Mukherjee, A.; Tothadi, S.; Desiraju, G. R. *Acc. Chem. Res.* **2014**, *47*, 2514. (b) Tothadi, S.; Joseph, S.; Desiraju, G. R. *Cryst. Growth Des.* **2013**, *13*, 3242. (c) Bui, T. T. T.; Dahaoui, S.; Lecomte, C.; Desiraju, G. R.; Espinosa, E. *Angew. Chem., Int. Ed.* **2009**, *48*, 3838.